LOAD FLOW MODEL FOR DROOP-CONTROLLED ELECTRIC SYSTEMS

CASE OF MICROGRIDS

Tayeb Meridji

A Thesis

in

The Department

of

Electrical and Computer Engineering

Presented in Partial Fulfillment of the Requirements

for the Degree of Master of Applied Science at

Concordia University

Montreal, Quebec, Canada

September, 2016

CONCORDIA UNIVERSITY
SCHOOL OF GRADUATE STUDIES

This is to certify that the thesis prepared

By: Tayeb Meridji

Entitled: "Load Flow Model for Droop-Controlled Electric Systems: Case of Microgrids"

and submitted in partial fulfillment of the requirements for the degree of

Master of Applied Science

Complies with the regulations of this University and meets the accepted standards with respect to originality and quality.

Signed by the final examining committee:

_____ Chair
Dr. R. Raut

_____ External Examiner
Dr. Hua Ge (BCEE)

_____ Internal Examiner
Dr. A. Rathore

_____ Supervisor
Dr. L. A. Lopes

Approved by: _____
Dr. W. E. Lynch, Chair
Department of Electrical and Computer Engineering

_____20_____

_____
Dr. Amir Asif
Dean, Faculty of Engineering and
Computer Science

ABSTRACT

Microgrids are independent micro electric systems made up of locally controlled systems that can function both connected to the main grid (on-grid mode) or isolated from the main grid (off-grid or islanded mode). CIGRE defines Microgrids as "electricity distribution systems containing loads and distributed energy resources, (such as distributed generators, storage devices, or controllable loads) that can be operated in a controlled, coordinated way either while connected to the main power network or while islanded."

As described by the IEEE Standards Coordinating Committee, microgrids have the ability to: (1) improve electrical reliability for customers; (2) relieve electric power system overload problems, in particular for highly congested power systems; and (3) resolve power quality issues. Most of the advantages offered by microgrids heavily rely on their predisposition to operate in isolated, independent mode. However, microgrids in islanded mode present technical operating challenges that need to be thoroughly investigated.

A microgrid must be able to independently meet the active and reactive power requirements of its assigned loads. In addition, it must also actively regulate voltage and frequency within a safe operating range in order to ensure system stability.

Investigating the technical challenges of islanded microgrids requires appropriate modeling tools. As is the case for high voltage (HV) power systems, the reliability of an isolated microgrid starts with a thorough investigation of its behaviour under various steady-state conditions and a derivation of the steady-state voltage profiles and transmission line loading levels throughout the system.

The present thesis investigates the steady-state analysis of islanded microgrid systems. To that end, an algorithm is developed using MATLAB to solve positive sequence (i.e., balanced) load-flow problems associated with isolated microgrids (IMGs). The proposed algorithm takes into account the specificities of IMGs and therefore yields more accurate results than those obtained with a conventional load flow algorithm. Compared to a conventional load flow algorithm, the algorithm that is most suitable for IMG has the following salient features: (1) no slack bus capable of supplying/absorbing the deficit/excess active and reactive power, (2) variable system frequency, and (3) part of, if not all, DG units operated in droop-control mode, which means that their active and reactive power outputs are not pre-specified, but are rather dependent on load flow variables (i.e., system frequency and bus voltages, respectively) at a given time.

ACKNOWLEDGEMENTS

I would like to greatly thank Dr. L. Lopes, from whom I have considerably benefited all along my work on the thesis. His valuable guidance allowed me to become more knowledgeable about microgrids and their operation. I would also like to thank all members of my family whose moral support was of inestimable value throughout this journey.

TABLE OF CONTENTS

LIST OF TABLES

LIST OF FIGURES

ACRONYMS

GS	Gauss-Seidel
NR	Newton-Raphson
CGS	Conventional Gauss-Seidel method
DER	Distributed Energy Resource
DG	Distributed generation unit
HV	High Voltage
IMG	Islanded Microgrid
LV	Low Voltage
MG	Microgrid
MGS	Modified Gauss-Seidel method
MV	Medium Voltage
OPF	Optimal power flow
PC	Point of coupling
PCC	Point of common coupling
PF	Power flow
PWM	Pulse-Width Modulation

VARIABLE DEFINITION

i_o	DG unit output current at the PCC
I_{ij}	Magnitude of the current flowing in the line between buses i and j
P_{Gi}, Q_{Gi}	Active and reactive power output at bus i, respectively
P_{Gi_max}, Q_{Gi_max}	Maximum active and reactive power output of generators at bus i, respectively
Vi_0, ωi_0	Reference output voltage magnitude and frequency of droop-controlled DG unit at bus i, respectively
Vi	Voltage magnitude at bus i
V_{i_max}	Maximum acceptable voltage
V_{i_min}	Minimum acceptable voltage
Ω	Steady-state frequency of the microgrid
ω_{max}	Maximum acceptable steady-state frequency
ω_{min}	Minimum acceptable steady-state frequency
n_q	Reactive power static droop gain
m_p	Active power static droop control
Y	Impedance matrix

K_{pf}	Active power load sensitivity to frequency changes
K_{qf}	Reactive power load sensitivity to frequency changes
α, β	Coefficients to reflect the type of loads (residential, commercial, or industrial)
n_{bus}	Total number of buses
n_{droop}	Total number of droop-controlled buses
n_{PV}	Total number of PV-type buses
n_{PQ}	Total number of PQ-type buses

CHAPTER 1

INTRODUCTION

1.1 Motivation

As the infrastructure of the existing centralized electric system ages and further deteriorates, a paradigm shift in electricity generation and transmission is emerging in developed countries, most notably in Europe, North America, and Japan. Power transmission systems of the majority of these countries are under escalating pressure as the problem of high voltage (HV) transmission line congestion is both increasing the cost of power delivery and degrading existing HV transmission lines and equipment by operating them at the limits of their maximum loading capabilities. With electricity demand expected to double in the next 20 years [1] and environmental considerations making it more difficult to obtain the necessary right-of-ways for new transmission corridors, finding alternative ways to meet future power demands without necessarily resorting to new transmission lines connecting generation centers to geographically distant load centers, becomes urgent. In this context, microgrids are pivotal elements in this new, emerging paradigm that is meant to circumvent some of the limitations of the existing power system. In reality, the latter paradigm is pushing the power sector away from centralized integration into more dispersed organization in which sources and sinks are clustered into semiautonomous microgrids.

In the context of their integration into the main grid, microgrids provide the following major benefits:

- Overall reliability improvement: Ultimately, a significant portion of the electrical system will be composed of self-sufficient "pockets" that could run without the support of the main grid. The possible autonomous operation of microgrids allows them to meet the demand of their associated loads even when the main grid is not available. Therefore, the commonly resorted to load-shedding operations (to avoid a drop in system frequency, or loss of synchronism, of the main electric system under contingency operation) is reduced [2].
- Main grid support: When the microgrid is in on-grid mode, it has the possibility of selling its excess power to the main grid. This feature greatly benefits the main grid, especially at peak demand, and further allows an increase of its available spinning reserve [3].
- Reduction of the main grid's overall transmission losses: Microgrids are primarily destined to supply end-users in situ. This approach has the merit of drastically reducing the non-negligible losses usually incurred on long HV transmission lines. The reduction of transmission losses (which, on a typical high voltage transmission line, amount to approximately 5 to 10 % of the total conveyed power) translates into a significant decrease in the overall cost of electricity.

As evidenced by the above benefits, in the new paradigm, main grid benefits are optimal when integrated microgrids have the capability of operating in islanded, off-grid mode. Nevertheless, operating microgrids in islanded mode presents a great many technical challenges that need to be addressed before the potential merits of microgrids are fully

derived. As detailed in IEEE 1547.4, the core of these technical challenges is comprised of the following issues:

- Having the ability to regulate the voltage and frequency within the agreed upon operating ranges.
- Providing the real and reactive power requirements of the loads within the island.
- Ensuring the availability of an adequate reserve margin within the microgrid. This reserve margin is typically a function of the load factor, the magnitude of the load, the load shape over time, the reliability requirements of the load, and the availability of the distributed generators.

Load flow analyses are performed to investigate the different technical aspects listed above. However, although the load flow problem is a fairly mature subject, conventional algorithms lack the ability to mimic the operating philosophy of islanded microgrids. Further, using time domain simulation tools to conduct load flow studies (i.e., studies meant to primarily investigate overloading and steady-state voltage instability problems) is time consuming and therefore inefficient.

Efficient tools must therefore be available in order to study microgrids and perform their associated planning studies. The present thesis presents a complete load flow algorithm capable of mimicking balanced microgrids operating in islanded mode. The proposed algorithm is based on the Gauss-Seidel method of solving non-linear equations.

1.2 Research Objectives

The main objective of this thesis is to develop new analysis tools for load flow problems pertaining to microgrids operated in balanced islanded mode.

1.3 Thesis Layout

The present thesis is organized as follows:

Chapter 2: Operation of Microgrids: Detailed description of the operation of microgrids. Salient features of these types of grids are also documented.

Chapter 3: Literature Survey: A review of the commonly used algorithm to study steady-state operation of microgrids. Further, current research conducted in the field of load flow for isolated microgrids are reported.

Chapter 4: Load Flow Algorithm for Balanced Islanded Microgrids: This chapter sets forth the modeling assumptions and the mathematical method that will used to solve the load flow problem for isolated microgrids.

Chapter 5: Simulation Results: This chapter discusses the results of the developed load flow algorithm.

Chapter 6: Conclusion and Future Work

CHAPTER 2

OPERATION OF MICROGRIDS

2.1 Introduction

For the last two decades, modern electric systems have been undergoing drastic changes insofar as a higher portion of their power demand is met by a higher number of distributed generation (DG) units. It is more and more common to see regions of the electric system with a sufficiently high number of DG units so as to form an independent cluster and thereby supply all or most of the power demand of the electric system's local assigned loads. These independent regions are referred to as microgrids.

A microgrid is a low-voltage (i.e., with a voltage ranging from AC 50V to 1kV) electric network principally comprised of three major components: loads, micro-sources in the form of distributed power generators (DGs), and relatively short transmission lines or feeders. Loads fed by microgrids can either be residential, commercial, or industrial. As for the micro-sources, they can be either conventional sources or renewables sources. Finally, the transmission lines and/or feeders of typical microgrids are relatively short in length and characterized by a non-negligible resistance component. For comparison purposes, Table 2.1-1 shows the typical characteristics of low, medium, and high voltage lines [4]. As can be observed, X/R ratios in a microgrid (LV system) are relatively low when compared to their HV counterparts.

Table 2.1-1 Typical Microgrid Line Parameters as Compared to Higher Voltage Systems

Type of Line	R (Ω/km)	X (Ω/km)	X/R
Low Voltage	0.642	0.083	0.13
Medium Voltage	0.161	0.190	1.18
High Voltage	0.060	0.191	3.18

All microgrids are designed to operate in either grid-connected mode or off-grid (islanded) mode. The conceptual design of a microgrid is shown in Figure 2.1-1. The microgrids can be seen as independent components of the main grid.

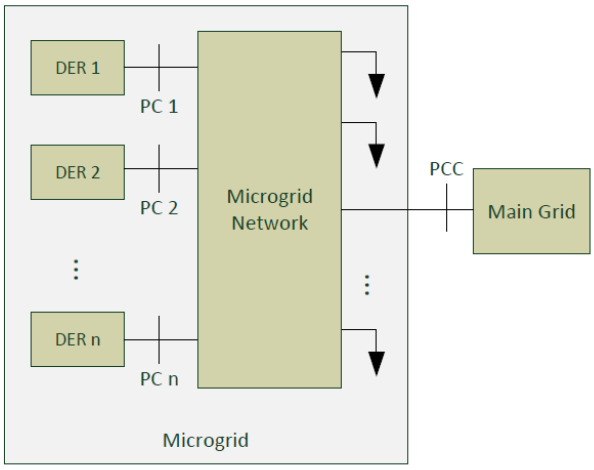

Figure 2.1-1 Conceptual Design of a Microgrid

Figure 2.1-2 provides a more detailed picture of a microgrid. This figure shows the location of the point-of-common-coupling as well as the circuit-breaker which, when opened, makes the

microgrid transition from grid-connected mode to islanded mode, that is to say that the microgrid operates independently and its loads are solely supplied by its micro-sources.

Energy generation sources in a microgrid are heterogeneous and can either be standard diesel generators, wind turbines, or solar panels. Given that the latter sources produce either dc or variable frequency electric power, electronic power converters (i.e., inverters) are necessary for coupling the microgrid to the ac grid [5]. Seen from the main grid, an inverter-interfaced DG unit is an actively controlled voltage source connected through an impedance.

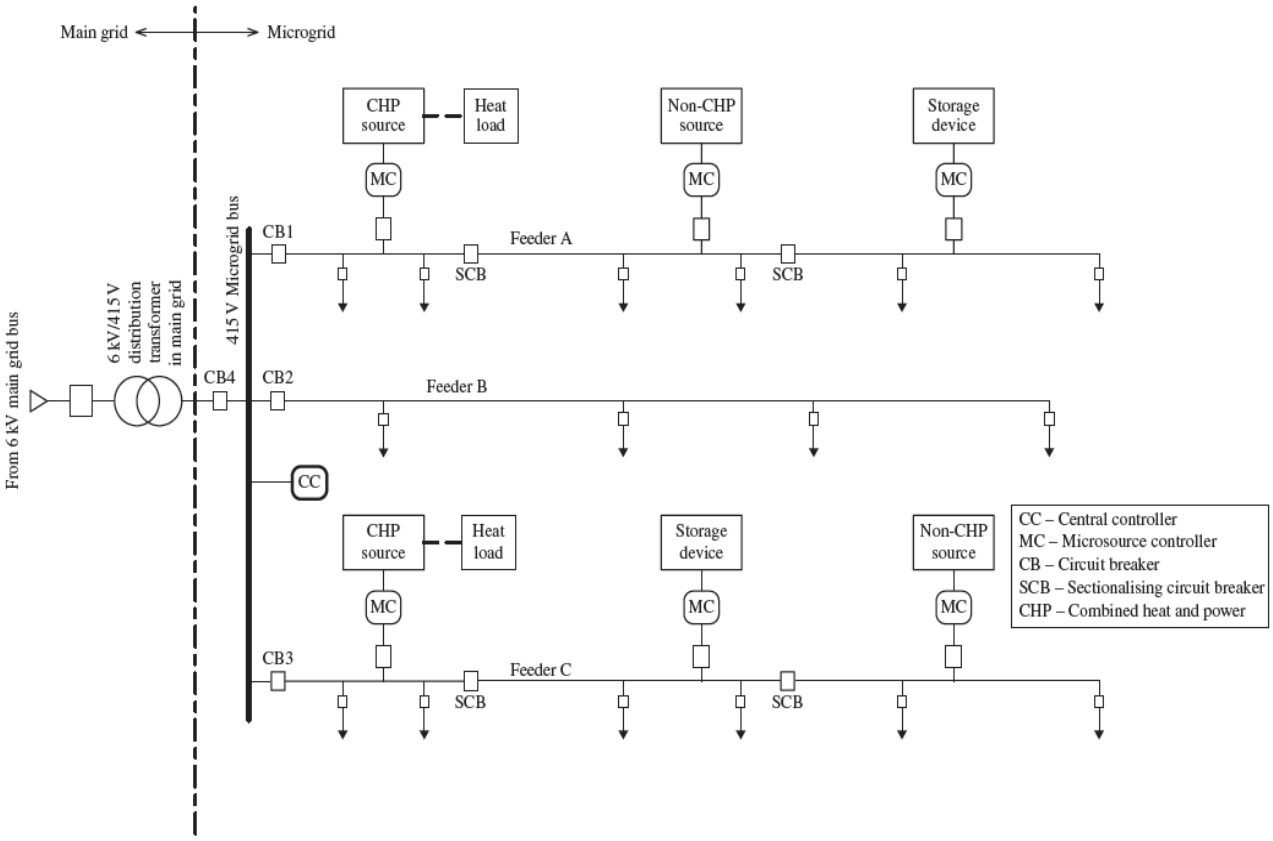

Figure 2.1-2 Typical Configuration of a Microgrid [6]

During on-grid operation, the main grid ensures that the microgrid operates within the acceptable frequency and voltage ranges. The main grid absorbs/injects the excess/deficit active or reactive power from the microgrid, hence ensuring a balance between power demand and supply. When in on-grid operation, the microgrid tracks the frequency and phase of the prevailing grid voltage at the PCC. Further, in normal grid-paralleled conditions the microgrid can be operated in a variety of control modes: based-load, load power dispatch, etc. For example, when operating in based-load mode, a microgrid composed of inverter-interfaced DG units can be set to deliver a pre-specified level of power to the main grid at a constant power factor [7].

However, when operated in off-grid mode, the microgrid loses the reference bus at the PCC. Therefore, in off-grid mode the DG units of the microgrid must assume the role of controlling their active and reactive power supply to meet load demand since no slack bus is available anymore. Two approaches permit this control: centralized control or decentralized control. As will be seen later, a slack bus is usually the bus that is connected to the generator with the highest output power capacity. This typically allows the slack bus to compensate for any shortage or surplus of active and/or reactive power. In this context, a microgrid connected to the main grid "sees" the latter as a generator with infinite capacity.

Centralized control requires a central controller that is tasked with controlling all DG units of the microgrids. These units are normally controlled in a master-slave topology whereby the master DG unit (typically the largest unit in the microgrid) sets the reference voltage for the slave DG units. The amount of information shared between the DG units and the central control center requires that the communication channels have large bandwidths. The control algorithms used in

this control mode ensures optimal operation of the microgrid by optimizing renewable power input while maintaining system stability. However, the central control has several drawbacks, the most important of which are [8]:

- It has a single point failure, which means that an eventual malfunction of the central control system would lead to a system collapse, provided that the central control systems manages all the system's micro sources.
- Achieving redundancy of the central control center is expensive.
- It necessitates expensive large bandwidth communication channels due to the high quantity of information exchanged between the DG units and the central control center.
- The maintenance of the central control system requires complete shutdown of the microgrid.

The high dependency of a microgrid on a central control system increases its vulnerability and counteracts its sought-after distributed and independent nature. Therefore, centrally controlled microgrids do not necessarily improve the overall resilience of the main grid they are connected to.

Because of the inherent limitations of central control, microgrids are most of the time controlled in a decentralized fashion through individual controllers associated with DG unit. These individual controllers make use of the frequency of the system to "communicate." The modularity of the decentralized control mode gives it the following advantages [8]:

- Individual DG controllers provide control redundancy to the microgrid, ensuring that if one generator controller fails, the remaining generators will compensate for the loss of generation.
- The microgrid becomes more scalable and extendable.
- It is a more cost-effective solution.

It should also be noted that a low bandwidth communication channel can also be coupled with the decentralized control to achieve optimal system operation by adjusting certain system parameters to reduce the overall production cost of the microgrid.

In industry, decentralized control of microgrids is the norm and is based on droop control technique. Nevertheless, in an islanded microgrid, when a DG unit is operated in droop-controlled mode, the latter is able to control only the voltage at the point of coupling (PC) of the DG (i.e., the location where the DG unit is connected to the rest of the microgrid). However, ensuring that the voltage magnitude is controlled at the PCC does not guarantee that the voltage is within the permissible limits at downstream load buses. Indeed, voltage drops along the feeders, which connect the micro-sources to the loads, can be high enough to cause an under-voltage at the load. For that reason, decentralized control cannot be fully relied upon to ensure proper operation of a microgrid.

To palliate the downfalls of the decentralized control approach, the latter can be complemented with a microgrid control center (MGCC) to optimize the operation of microgrids and guarantee their operation within pre-specified acceptable limits. The MGCC takes into account technical

constraints throughout the microgrid and economic costs to operating the system. An MGCC operates as follows:

- Collects input data (mainly total generation and load) from different measurements points in the microgrid.
- Runs an optimal power flow to dispatch the in-service generators while maintaining voltage levels, loading level of feeders, and system frequency within acceptable limits. Control is achieved through the droop settings of the droop-control generators (i.e., either reference voltage, reference frequency, or the active and reactive power static droop gains).
- Once the new droop settings are calculated, they are communicated to each generate via a low-bandwidth communication link.

It is important to note that in the case where the MGCC fails to operate, the microgrid would still function, albeit not optimally.

The load flow algorithm developed in this thesis is based on the decentralized control philosophy of microgrids.

2.2 Droop Control Technique

The primary control objective in a microgrid is to achieve accurate power sharing between its generators and other micro-sources while meeting its load demand and maintaining its voltage and frequency constant. By combining decentralized control and droop control, each controller associated with a DG unit aims at mimicking the behaviour of a synchronous generator. In this

manner, it could be said that the conventional large grid control concept is down scaled to the level of microgrids.

In systems that are predominantly composed of rotating generators, such as microgrids, frequency and active power are closely related entities. Moreover, inverter-interfaced DG units have the same behaviour as rotating generators with respect to active and reactive power generation, as well as terminal voltage control. Increasing the amount of load increases the load torque. If the prime mover torque of the rotating generator feeding this load is not proportionally increased, its rotating speed, and hence the frequency of the system, drops.

The same principle applies for a synchronous generator. If the generation is not adequately adjusted to cover the extra load demand when its associated load increases, the frequency decreases. Similarly, when the load decreases, the frequency increases if the generation is not accordingly decreased. This exact behaviour is reproduced by means of the droop control technique. Adjusting the frequency in accordance to the changes in the load is the primary role of droop control. The frequency is used to control the supplied active power, while the voltage magnitude is used to control the amount of injected reactive power.

2.3 Droop Control Implementation

In order to understand the equations governing the droop control method, the simplified microgrid circuit of Figure 2.3-1 is considered. This microgrid is composed of two DG units radially feeding a load via two feeders. The voltages of the inverter-interfaced DG units are respectively $\overline{V1}$ and $\overline{V2}$, while the voltage at the point of common coupling is denoted by $\overline{Vp}$.

In the following derivations, it is assumed that the output impedance of the DG-interfacing converters (i.e., the converter which interfaces the DG unit with the microgrid system) is predominantly inductive. Therefore the combined LC filter and line impedance will also be predominantly inductive. Hence, line resistances can be neglected without loss of accuracy.

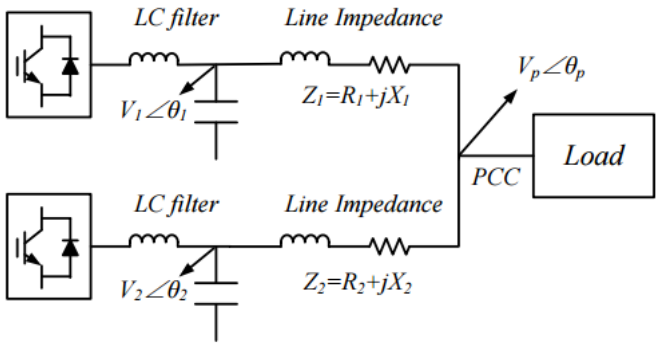

Figure 2.3-1 Simplified Circuit of a Microgrid [9]

In its simplified form, the active and reactive power flowing from one DG Unit to the PCC can be written as follows, with x denoting the number of the DG unit [10]:

$$P_x = \frac{V_x * V_p}{X_x} * \sin\theta_{xp} \qquad (2.1)$$

$$Q_x = \frac{V_x * (V_x - V_p * \cos\theta_{xp})}{X_x} \qquad (2.2)$$

If the power angle between the two extremities of a feeder is small (which is typically the case), then the small angle formula can be used, so that $\sin\theta \cong \theta$ and $\cos\theta \cong 1$. Therefore, the above two equations for active and reactive power can be written as follows:

$$\theta \cong \frac{X_x * P}{V_x * V_p} \qquad (2.3)$$

$$V_x - V_p = \frac{X_x * Q}{V_x} \qquad (2.4)$$

From these simplified power transfer equations, it can be seen that active power flow depends heavily on the phase angle difference between the sending and receiving end, while reactive power flow depends on the voltage (magnitude) difference between the two ends of the feeder. In droop control, frequency rather than phase angle is used to control active power flow. Based on these observations, the common droop control equations can be derived:

$$w = w_0 - m_p * P \qquad (2.5)$$

$$V = V_0 - n_q * Q \qquad (2.6)$$

Where w_0 and V_0 are respectively the reference angular speed and voltage. Coefficients m_p and n_q, on the other hand, are the active and reactive power static droop gains. These gains specify the slope of the droop characteristic and hence control the reactivity speed of a droop-controlled DG unit to changes in either frequency or voltage, that is, how fast the control should react to a change in either system frequency or bus voltage magnitude. The typical droop control characteristic diagrams are depicted in Figure 2.3-2, which shows that beyond the maximum active and reactive power limit of the DG unit, the output of the DG unit is set to that its maximum bounding limit. The same reasoning applies to the minimum limits, when they exist.

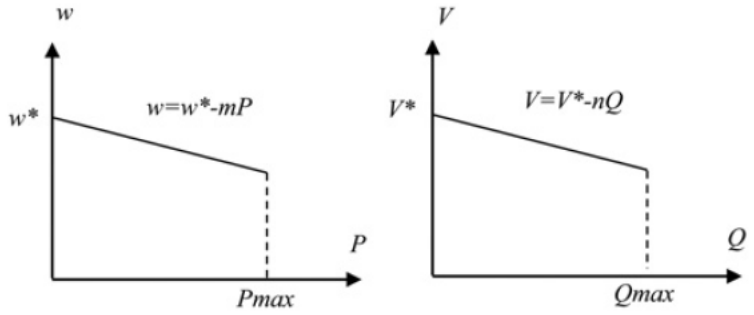

Figure 2.3-2 Static Droop Characteristics [11]

Figure 2.3-3 depicts the typical diagram of the power circuit in addition to the control circuit of a droop-controlled DG unit that is operating off-grid [12]. The implementation of droop control necessitates local measures of both voltage and current at the terminal of the inverter-interfaced DG unit. The interfacing inverter is also equipped with an LC filter that is used to eliminate the switching harmonics generated by the converter unit.

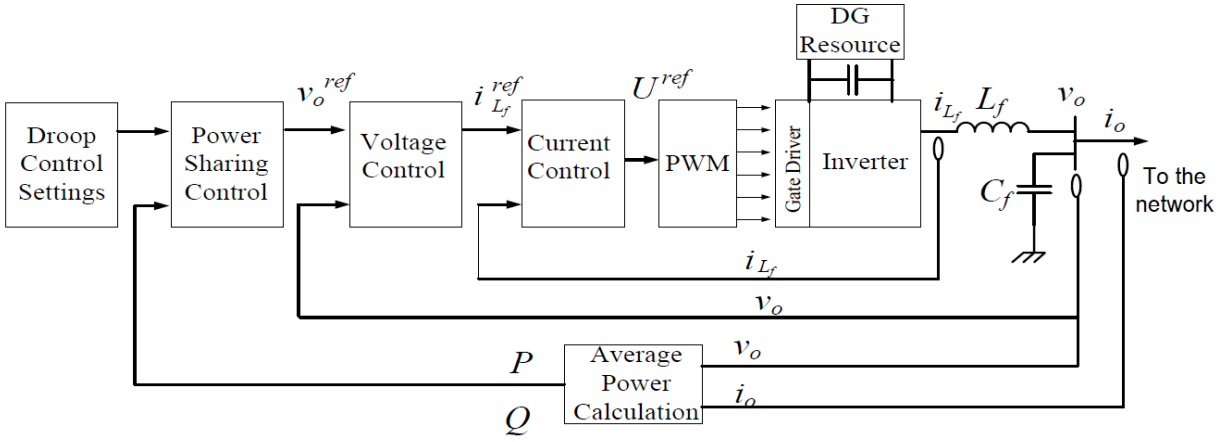

Figure 2.3-3 Control structure of a droop-controlled DG unit

CHAPTER 3

LITERATURE REVIEW

3.1 Need for Power Flow Algorithms for Microgrids

In order to deploy and operate a microgrid safely, planning studies should be conducted to test weaknesses of the system. Of particular interest are voltage stability studies that look at the variation of voltage throughout the microgrid as the load and operating conditions vary. In addition, knowing the fluctuation of system frequency with respect to changes in load is also paramount in the design of microgrids.

It is common practice to use time-domain simulations tools (such as PSCAD or MATLAB) to conduct such studies for the particular case of microgrids. Although these tools are very accurate, given that their associated algorithms solve a set of differential equations which describe the system response at every sampling time, overall required computational time is extremely long. In addition, since a large level of detail is required for constructing such time-domain models, only small-scale systems can be simulated. All these limitations call for a much simpler load flow algorithm that is able to mimic the operation of an islanded microgrid under steady-state conditions.

In much of the available literature, conventional load flow algorithms have been widely used to model islanded microgrids. However, this approach discards major differences between a power system grid and a microgrid. More specifically:

- In a microgrid there is no slack bus which is able to compensate for the mismatch between the generated and the consumed active and reactive powers since a microgrid is typically composed of relatively small and equal-sized DG units that cannot assume the role of a slack generator.
- In conventional load flow problem formulations, the steady-state frequency of the system is assumed to be constant. This assumption is problematic in microgrids again because of the lack of a slack bus capable of supplying/absorbing the excess/deficit of active power to ensure a constant frequency. Therefore, in the microgrid formulation of the load flow problem, the frequency of the system is an additional variable that needs to be solved.
- In a microgrid, buses to which are connected droop-controlled DG units cannot be modeled as PV buses since the output power of these units is proportionally adjusted to changes in system frequency.

Due to these conceptual errors in current practices, a load flow specifically tailored for isolated microgrids is necessary to conduct viable steady-state simulations.

3.2 Existing Work

In recent years, a number of research works have been conducted in the field of microgrids. In a great many number of them, for load flow calculation purposes, the islanded microgrid was simulated under steady-state conditions using conventional load flow algorithms [13, 14]. In the latter work DG units were modelled as either PV or PQ buses, whereas the DG unit with the highest power capacity was chosen as the slack unit. This, of course, leads to inaccurate results,

since the operation of a droop-controlled DG unit is very much different from that of a DG unit operating in PV or PQ mode, since the former is frequency-dependent while the latter is not.

More recently, two works have addressed the specific problem of load flow algorithms tailored for islanded operation of microgrids [15, 16]. In the work presented in [15], a load flow algorithm was developed to solve load flow problems of islanded unbalanced microgrids. The nonlinear load flow equations were solved using the Newton-Trust region method, which is a powerful method for solving nonlinear equations and large scale optimization problems. Although this method is very accurate, its implementation is relatively complex and is more suitable for very large power systems.

In another recently published work a simpler load flow algorithm was developed for islanded balanced microgrids [16]. It used the simpler Gauss-Seidel method to solve the nonlinear equations of the load flow problem. Nevertheless, the proposed algorithm was not tested for system operation under low frequency levels.

It should be mentioned that in a number of other academic works, the islanded microgrid was simulated using time-domain simulation tools, such as PSCAD. These types of simulations, although very accurate, are time-consuming in the modeling phase and therefore inadequate for conducting system planning studies.

3.3 Discussion of Needs

The conducted literature review shows that steady-state operation of microgrids is still being extensively studied using time-domain simulation tools or simply conventional load flow algorithms. The previous paragraphs demonstrated the shortfalls of each of these approaches. Time-domain simulations are computationally expensive while conventional load flow algorithms do not capture the real steady-state behaviour of microgrids operated off-grid.

It was also shown that the approach followed in [15] was too complex to be easily implemented, as it relied on a rather sophisticated mathematical formulation which is more convenient for simulation involving very large electric systems. The simpler approach adopted in [16] is much simpler than the preceding method but it still needs to be tested for systems operating at relatively low system frequencies. It shall be noted that the latter low frequency test was not conducted in [16] and therefore it cannot be fully conclude that the method can be used to emulate islanded microgrids.

In light of these needs, the purpose of this thesis is to develop a simple yet accurate algorithm for the modeling of steady-state operation of isolated microgrids. In addition to the nominal system frequency operation, the developed algorithm will be specially tailored to also tackle reduced frequency operation[1] without running into non-convergence problems.

[1] Reduced frequency operation is defined as microgrid operation at frequencies around 0.95pu of the nominal frequency.

CHAPTER 4

LOAD FLOW ALGORITHM FOR BALANCED ISLANDED MICROGRIDS

4.1 Introduction

There is a need to develop a load flow algorithm adapted to the behaviour of isolated microgrids since conventional load flow algorithms do not yield accurate results when applied to isolated microgrids, for the following reasons:

- Absence of a slack bus.
- Fluctuation of the frequency, which makes it another variable of the load flow problem.
- Operation of a number of DG units in droop controlled mode. Therefore the bus to which these generators are connected can no longer be defined as PV buses.
- Variation of the impedance matrix with respect to frequency. This results in the variation of the impedance matrix at each iteration of the LF algorithm.

The present section is organized as follows:

1. **Conventional load flow problem**: presents the load flow problem in its conventional form: types of buses and mathematical formulation.
2. **LF problem formulation applicable to isolated microgrids**: presents the peculiarities of islanded microgrids that need to be accounted for in the general formulation of the load flow equations. This section aims at showing the major

differences between conventional load flow problems and isolated microgrid problems.

3. **System modeling of microgrids**: presents the mathematical equations used to model each component of a microgrid: load, feeders, DG units.
4. **Gauss-Seidel method**: presents the theoretical background behind the Gauss-Seidel method for solving non-linear equations. The Gauss-Seidel method is used in this thesis to solve the set of non-linear equations that define the load flow problem.
5. **Gauss-Seidel method applied to load flow problems in isolated microgrid**: presents the necessary modifications needed to adapt the Gauss-Seidel method to the load flow problem of isolated microgrids.

4.2 Load Flow Problem Presentation

4.2.1 Conventional Load Flow Problem

The main purpose of a load flow analysis is to evaluate the match between generation and load. The load flow problem is the mathematical description of the relations between the various components of the overall power system network. More specifically, the load flow problem involves the computation of voltage magnitudes and phase angles at each bus in a power system under balanced three-phase steady-state operation. Once the latter quantities are evaluated, the active and reactive power flows through system element, such as transmission lines and transformers, can be deduced. The outcome of this analysis is generally used for the evaluation of steady-state, as well as dynamic performance, of interconnected electric systems.

The relationship between (a) voltage and current at each bus, (b) real and reactive power demand at a load bus, as well as (c) generated real power and scheduled voltage magnitude at a generator bus is non-linear in nature. This non-linearity is due to the fact that the power flowing into any given load impedance in the system is a function of the square of the applied voltage at the bus of interconnection. Therefore, power flow calculations require solving a set of non-linear equations in order to derive the electric response of the transmission system under a specific set of conditions characterized by load level and generation.

The current section provides an overview of the power-flow analysis of a conventional large network. At a subsequent stage, the adjustments needed to adapt the conventional power-flow problem formulation to the analysis of an islanded microgrid will be detailed. Given that the system is assumed to be balanced, a single phase representation of the system is made possible and will be assumed throughout the analysis.

4.2.1.1 Mathematical Formulation of Conventional Load Flow Problems

Considering a system with *n* independent buses, applying Kirchhoff's law at each bus yields the following *n* equations [17]:

$$\begin{aligned} Y_{11}\mathbf{V_1} + Y_{11}\mathbf{V_2} + \cdots + Y_{1n}\mathbf{V_n} &= \mathbf{I_1} \\ Y_{21}\mathbf{V_1} + Y_{22}\mathbf{V_2} + \cdots + Y_{2n}\mathbf{V_n} &= \mathbf{I_2} \qquad (4.1) \\ \cdots & \\ Y_{n1}\mathbf{V_1} + Y_{n2}\mathbf{V_2} + \cdots + Y_{nn}\mathbf{V_n} &= \mathbf{I_n} \end{aligned}$$

Where,

$\mathbf{I} \triangleq$ bus current injection vector

$\mathbf{V} \triangleq$ bus voltage vector

$\mathbf{Y} \triangleq$ admittance matrix

$Y_{ii} \triangleq$ the diagonal element of the bus admittance matrix

$Y_{ij} \triangleq$ the off diagonal element of the bus admittance matrix

Notes:

- Y_{ii} refers to the self-admittance of bus I and equals the sum of all branch admittances connecting to bus I, that is: $y_{i0} + y_{i2} + \ldots + y_{in}$. It shall be noted that y_{i0} is the total capacitive susceptance at bus i.
- Y_{ij} is called the mutual-admittance of bus i. It equals the negative value of the branch admittance between buses i and j.
- The off-diagonal element of the admittance matrix is equal to zero when there is no branch (i.e., transmission line) between buses i and j.

The bus current can be written in terms of bus voltage and apparent power as follows:

$$\mathbf{I_i} = \frac{\mathbf{S_i^*}}{\mathbf{V_i^*}} = \frac{P_{(net)i} - j * Q_{(net)i}}{\mathbf{V_i^*}} \qquad (4.2)$$

Where,

$\mathbf{S} \triangleq$ the apparent complex power injection vector

$P_{(net)i} \triangleq$ the net real power injected at bus i $(P_{Gi} - P_{Li})$

$Q_{(net)i} \triangleq$ the net real power injected at bus i $(Q_{Gi} - Q_{Li})$

$$\frac{P_{(net)i}-j*Q_{(net)i}}{V_i^*} = Y_{i1}\mathbf{V_1} + Y_{i2}\mathbf{V_2} + \cdots + Y_{in}\mathbf{V_n} \quad (4.3)$$

Or,

$$P_{(net)i} - j * Q_{(net)i} = \mathbf{V_i} \sum_{j=1}^{n} Y_{ij}{}^{*}\, \mathbf{V_j}^{*} \quad (4.4)$$

By equating the real and imaginary part of the above expression, two equations for each bus are derived in terms of four variables: P, Q, V, and the angle θ.

Using the Gauss-Seidel numerical method (detailed in a subsequent section of this report), the above equation for active and reactive power is solved.

4.2.1.2 Classification of buses

The first step in resolving the load flow problem consists of defining the type of buses. Three types of buses exit in conventional LF problems:

- PQ buses (or load buses): both P and Q are known; V and delta are unknown.
- PV buses (or generator buses): also known as Voltage Controlled buses, where P and V are known; Q and delta are unknown. At these buses the active output power of the generator as well as its terminal voltage are set to a fixed value. With varying system conditions, the reactive power output of the generator is adjusted to keep the terminal voltage of the generator at its scheduled value.
- Slack buses: in the formulation of a load flow problem one slack bus is always defined. This bus can be seen as the variable of adjustment of the active and reactive power circulating in the system; the slack bus supplies the difference between the scheduled real

power generation and the sum of all loads and system losses. It is common practice to have the largest generator in the network assume the role of slack. At the slack bus, V and delta are known (assumed to be 1 pu and 0 degrees, respectively); P and Q are unknown.

After solving the load flow problem, the difference between the total calculated power going into all buses and the total power output of all generators plus the losses are assigned to the slack bus. Given that a constant frequency is assumed, the amount of generated power must always be equal to the consumed power.

4.2.2 Unconventional Load Flow Problem: Case of Islanded Microgrids

When in grid-connected mode, the frequency and voltage stability of the microgrid is ensured by the grid, which is seen at the point of common coupling as an infinite (slack) bus capable of supplying/absorbing the deficit/extra power associated with the microgrid. Under grid-connected mode, the LF problem for the microgrid is formulated in the same way as the conventional LF problem.

However, when the microgrid is operated in the islanded mode, modifications are necessary to solve the LF problem. Indeed, when in islanded mode, no microgrid bus can be assumed to be an infinite bus with the capacity of supplying/absorbing the deficit/extra active and reactive power circulating in the system. A stricter control and share of active and reactive power between the micro-sources of the microgrid is therefore necessary.

As previously stated, the control of microgrids can either be centralized or decentralized. The centralized mode necessitates the availability of a telecommunication infrastructure to ensure the

centralized control of all generators. The latter mode of control generally proves impractical and economically unappealing for small microgrids in remote areas. For that reason, the most common control mode is the decentralized droop control mode, also known as wireless control. The next section discusses the details of the modeling of each microgrid component, specifically the loads, generators, and feeders.

4.3 System Modeling of Microgrids

The present section details the mathematical representation of each element of a microgrid.

4.3.1 Load Modeling

In a microgrid, the mathematical expression that represents the load must account for the variation of both the absorbed active and reactive power with respect to a variation in terminal voltage magnitude and system frequency. The amount of active and reactive power absorbed by a load can be calculated using the following formulae [15]:

$$P_{Li} = P_{oi} * |Vi|^{\alpha} * \left(1 + K_{pf} * \Delta\omega\right) \qquad (4.5)$$

$$Q_{Li} = Q_{oi} * |Vi|^{\beta} * \left(1 + K_{qf} * \Delta\omega\right) \qquad (4.6)$$

Where,

$$\Delta\omega = \text{angular frequency deviation (pu)}$$

$$K_{pf} = \text{ranges from 0 to 3.0}$$

$$K_{qf} = \text{ranges from} -2.0 \text{ to 0}$$

P_{oi} and Q_{oi} are respectively the nominal active and reactive of the load. The factors K_{pf} and K_{qf} capture the sensitivity of the load to frequency changes [18]. $\Delta\omega$ is the angular frequency

deviation. And finally, coefficients α and β reflect the load type, be it a residential, a commercial, or an industrial type.

Table 4.3-1 shows typically used values for α and β [18].

Table 4.3-1 Exponents values per load types

Load Type	α	β
Constant Power	0.00	0.00
Constant Current	1.00	1.00
Residential	0.92	4.04
Commercial	1.51	3.40
Industrial	0.18	6.00

4.3.2 Y_{bus} Modeling

Y_{bus} is the admittance matrix of the microgrid. This matrix indicates the admittances of all transmission lines or feeders within the system. Given that the frequency is power flow dependent in an isolated microgrid, the line impedances can no longer be assumed constant. Indeed, the reactance component of the line impedance, ω*L, varies with changes in the frequency of the microgrid. It therefore follows that the admittance matrix Y_{bus} can no longer be assumed constant. The following matrix has the typical form of admittance matrices used in power flow calculations.

$$Y_{bus} = \begin{bmatrix} Y_{11}(\omega) & \cdots & Y_{1n}(\omega) \\ \vdots & \ddots & \vdots \\ Y_{n1}(\omega) & \cdots & Y_{nn}(\omega) \end{bmatrix} \qquad (4.7)$$

Where $Y_{ij}(\omega)$ is interpreted as the admittance between bus i and bus j.

4.3.3 DG Units Modeling

Distributed generation (DG) is a term used to characterize a wide range of power generating units, most notably small diesel generators, wind turbines, and solar panels. It is common practice to connect wind turbines and solar panels to the microgrid through a DC to AC converter. The latter converter allows fixing the output power while maintaining a close to constant voltage by varying the reactive power generation of the unit.

When a microgrid is connected to the main grid, DG units are typically represented in the conventional load flow problem as either PV or PQ buses. This is because when in grid-connected mode, the frequency of the microgrid is controlled by the main grid. When a microgrid is islanded, however, DG units are operated so as to (a) supply the loads with the consumed power, and (b) regulate the voltage and frequency of the microgrid. In the absence of a slack bus, it becomes impossible to make all DG units operate in PV or PQ modes. Therefore, in islanded microgrids, DG units can be operated in any of the following three modes: PV, PQ, or Droop-based. For DG operating in the PV mode, the unit supplies a pre-specified amount of active power while the supplied reactive power is adjusted to achieve a pre-specified voltage value. For DG operating in the PQ mode, the unit injects pre-specified values of active and reactive power. Under this mode, the DG unit acts as a negative load. Finally, when the DG unit operates in the droop mode, the amount of active and reactive power generated by the unit depends respectively on the system frequency and the terminal voltage.

The following two equations, 4.8 and 4.9, show the relationship that exists between frequency and power, on one hand, and between voltage and reactive power on the other.

Figure 4.3-1, on the other hand, shows a DG unit (which is typically composed of the energy resource, the power electronics converter and its associated filter) is modeled as a droop-controlled ideal voltage source [8].

It is worth mentioning that the validity of the following two equations presupposes that the output impedance of the converter (interfacing between the DG and the microgrid) is predominantly inductive [19]. This is generally the case due to the large inductor used at the converter output along with the large inductor of the associated filters [20].

$$\omega = \omega_0 - m_p * P_{Gi} \qquad (4.8)$$

$$V = V_0 - n_q * Q_{Gi} \qquad (4.9)$$

Where,

$$V_0 = \text{nominal voltage}$$

$$n_q = \text{reactive power static droop gain}$$

$$\omega_0 = \text{nominal frequency setpoint}$$

$$m_p = \text{active power static droop gain}$$

$$m_p = \left(\frac{\omega_{max} - \omega_{min}}{P_{Gmax}}\right) \qquad (4.10)$$

$$n_q = \left(\frac{V_{max} - V_{min}}{Q_{Gmax}}\right) \qquad (4.11)$$

The choice of the minimum and maximum allowable voltage and frequency should be chosen in such a manner as to ensure that the resulting voltage and frequency deviations are within the agreed upon ranges [21].

It is advised, although not mandatory, to have an equal sharing of power (active and reactive) of the DGs within a microgrid. When all DGs have the same maximum power ratings, the static droop coefficient will be the same as well. However, when the DGs have different ratings, the following equalities must be satisfied when selecting the static droop coefficients:

$$m_{p1}\, P_{g1,max} = m_{p2}\, P_{g2,max} = \ \ldots = m_{pi}\, P_{gi,max} \tag{4.12}$$

$$n_{q1}\, Q_{g1,max} = n_{q2}\, Q_{g2,max} = \cdots = \ n_{qi}\, Q_{gi,max} \tag{4.13}$$

Where *i* denotes droop-controlled buses.

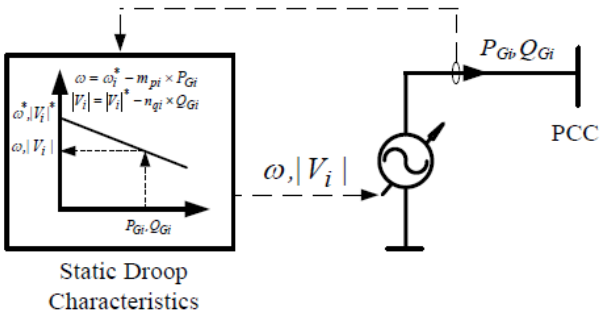

Figure 4.3-1 Generator Operated in Droop-Control Mode [15]

Now that the modeling of each component of microgrids has been discussed in detail, the next section examines the mathematical method used to solve the set of non-linear equations which describe the load flow problem as it presents itself for isolated microgrids, that is the Gauss-Seidel method.

4.4 Gauss-Seidel Method

4.4.1 Theory

The Gauss-Seidel method, or the method of successive replacement, is an iterative method widely used for solving non-linear equations of the form **Ax** = **b**. It proceeds by computing a sequence of progressively accurate iterates to approximate the closest solution of the set of linear equations. The Gauss-Seidel method is an improved version of the Jacobi iteration method. Consider a system given by the following equations:

$$a_{11}x_1 + a_{12}x_2 + \ \ldots + \ a_{1n}x_n = b_1$$

$$a_{21}x_1 + a_{22}x_2 + \ \ldots + \ a_{2n}x_n = b_2 \qquad (4.14)$$

...

$$a_{n1}x_1 + a_{n2}x_2 + \ \ldots + \ a_{nn}x_n = b_n$$

The final solution of this system can be written as:

$$\mathbf{x} = (x_1, x_2, x_3, \ldots, x_n) \qquad (4.15)$$

If the coefficient matrix **A** has non-zero elements on its main diagonal (that is, a_{11}, a_{22}, …, a_{nn} are non-zero) the following equations can be written:

$$x_1 = \frac{1}{a_{11}} * (b_1 - a_{12}x_2 - \ \ldots - \ a_{1n}x_n)$$

$$x_2 = \frac{1}{a_{21}} * (b_2 - a_{21}x_1 - \ \ldots - \ a_{2n}x_n) \qquad (4.16)$$

...

$$x_n = \frac{1}{a_{nn}} * (b_n - a_{n1}x_1 - a_{n2}x_2 \ \ldots - \ a_{n,n-1}x_{n-1})$$

The solution algorithm is started by making an educated initial guess of the solution of the first iteration, that is:

$$x(0) = (x_1(0), x_2(0), x_3(0), \dots, x_n(0)) \qquad (4.17)$$

These initial approximations are substituted into the right-hand side of the previous set of equations. The new values $x_i(k+1)$ are used in the next equation as soon as they are known. This means, for example, that once $x_1(k+1)$ has been computed from the first equation, its value is used in the second equation to evaluate $x_2(k+1)$, and so on. The latter computation process is described by the following equations:

$$x_1(k+1) = \frac{1}{a_{11}} * (b_1 - a_{12}x_2(k) - \dots - a_{1n}x_n(k))$$

$$x_2(k+1) = \frac{1}{a_{21}} * (b_2 - a_{21}x_1(k+1) - \dots - a_{2n}x_n(k)) \qquad (4.18)$$

...

$$x_n(k+1) = \frac{1}{a_{nn}} * (b_n - a_{n1}x_1(k+1) - a_{n2}x_2(k+1) \dots - a_{n,n-1}x_{n-1}(k+1))$$

The iteration process is carried on until the highest difference between a new approximation ($(x(k+1))$ and its previous approximation ($(x(k))$ is less than a pre-defined error ε.

4.4.2 Advantages and Disadvantages of the Gauss-Seidel Method

The most notable advantages of the Gauss-Seidel method in solving non-linear problems are the following:

- Simplicity.
- Small computer memory requirements.

- Less computational time per iteration.

However, the slow rate of convergence disadvantages this method and requires a large number of iterations to reach the final solution. Nevertheless, since the required number of iterations is proportional to the number of buses in the system, the Gauss-Seidel method appears to be appropriate for small scale microgrids.

4.4.3 Numerical Algorithm of the Gauss-Seidel Method

The following algorithm is used for the Gauss-Seidel method:

Input: A = $[a_{ij}]$, **b**, **XO** = $\mathbf{x}^{(0)}$, tolerance error TOL, Maximum number of iterations N.

Step 1: Set k = 1

Step 2: While (k ≤ N) do Steps 3 to 6

Step 3: For i = 1, 2, …, n

$$x_i = \frac{1}{a_{ii}} * [\sum_{j=1}^{i-1}(a_{ij}x_j) - \sum_{j=i+1}^{n}(a_{ij}XO_j) + b_i]$$

Step 4: if abs(**x** – **XO**) < TOL, then OUTPUT (x_1, x_2, x_3, …, x_n)

Stop Iterations

Step 5: Set k = k+1

Step 6: For i = 1, 2, …, n

Set $\mathbf{XO}_i = \mathbf{x}_i$

Step 7: OUTPUT (x_1, x_2, x_3, …, x_n)

Stop Iterations

4.4.4 Gauss-Seidel Applied to Microgrid Load Flow Problems

As shown previously, the load flow problem in an isolated microgrid is characterized by the following salient features:

- There is no slack bus.
- The system frequency is not constant.
- The matrix Y_{bus} varies with the fluctuation of the frequency.
- As the bus voltages vary, the power flowing through the lines varies, which signifies that the line losses are not constant.

It shall be mentioned that in order to minimize divergence problems of the modified load flow algorithm (i.e., the algorithm adapted to islanded microgrids), initial guesses of voltage and angle magnitudes are initially calculated using the conventional load flow algorithm. These initial guesses are then fed to the modified load flow algorithm. Without these close-to-reality guesses, divergence problems are encountered especially in the case where the microgrid is operated at relatively low system frequencies (say, around 0.95pu).

Three separate steps are necessary to solve the LF problem in a microgrid using the Gauss-Seidel method.

Step 1: Calculate the voltage at all buses and the system losses.

The voltage at all buses is calculated using the following expression:

$$\vec{V}_k^{i+1} = \frac{1}{\vec{Y}_{kk}} * [\frac{P_k - jQ_k}{(\vec{V}_k^i)^*} - \sum_{n=1}^{k-1}(\vec{Y}_{kn} * \vec{V}_n^{i+1}) - \sum_{n=k+1}^{N}(\vec{Y}_{kn} * \vec{V}_n^i)] \quad (4.19)$$

Where,

$$\vec{V}_k^{i+1} = \text{voltage for iteration } (i+1) \text{ at bus k.}$$

Equation 4.19 gives both voltage magnitude and voltage angle for the current iteration. It is worth noting that the algorithm requires the selection of a reference bus. When voltage is calculated for the selected reference bus, the resulting magnitude from equation 4.9 is kept while the angle is set back to zero. For droop-controlled buses, P_k and Q_k are estimated using equations 4.8 and 4.9, respectively[2]. For all PQ (or load) buses, P_k and Q_k are constant and readily known through equations 4.5 and 4.6. However, for PV buses, while the active power is known[3], the reactive power is evaluated using the following expression:

$$Q_k^{i+1} = -\text{Im}[(\vec{V}_k^i)^*(\sum_{n=1}^{k-1}(\vec{Y}_{kn} * \vec{V}_n^{i+1}) - \sum_{n=k}^{N}(\vec{Y}_{kn} * \vec{V}_n^i))] \quad (4.20)$$

For PV buses, two important facts should be kept in mind. First, once the reactive power generated at a PV bus is calculated, it must be verified to be within the Q limits of the unit. In case the calculated value lies beyond the maximum boundary, it must be set to Q_{max}. Secondly, when the voltage at the PV bus is evaluated, the new bus angle is kept while the magnitude is set

[2] If the calculated active or reactive power output of a droop-controlled generator is found to be higher that its output capacity, the output of that generator is accordingly set to its maximum or minimum limit.

[3] For PV buses (i.e., non-droop-controlled generator buses), both active power and bus voltage are constant and pre-selected.

back to its pre-defined value. For VF depend buses, droop equations can be used to evaluate the active and reactive power output.

Step 2: Calculate the new system frequency

Assuming that all DGs of the islanded microgrid are operating as droop based[4], it is inferred that the sum of all the active power generated by the DGs is equal to the total power circulating within the microgrid. In addition, given that the frequency is the same in the whole microgrid, droop controlled buses in the microgrid supply active power at the same angular frequency. Considering these observations, the following expression can be written:

$$P_{total} = P_{load} + P_{line\_losses} = \sum_{j=1}^{d} P_{Gk} = \sum_{j=1}^{d} \frac{1}{m_{pk}} (\omega_0 - \omega) \qquad (4.21)$$

From equation 4.21, system frequency can be derived as follows:

$$\omega^{i+1} = \frac{\sum_{j=1}^{d} \frac{1}{m_{pk}} \omega_0 - (P_{load}^{i+1} + P_{line\_loss}^{i+1})}{\sum_{j=1}^{d} \frac{1}{m_{pk}}} \qquad (4.22)$$

Where *d* denotes droop-controlled generators.

Step 3: Calculate the generated reactive power

The reactive power generated by the generators is evaluated and compared to the reactive power consumed by the loads. The total reactive power generated by droop-controlled generators can be derived from the expression relating the generative reactive power to both voltage mismatch,

[4] DC/AC or AC/AC inverters, which are widely used respectively to interface between solar and wind power units and the rest of the synchronous AC microgrid, are also commonly equipped with power-frequency droop controllers [4].

$V_{ref} - V_i$, and voltage droop coefficient, n_q. The reactive power generated at PV buses can be calculated using the expressions given in the previous section. The calculated new voltages must also satisfy the following expression to ensure that the reactive power demand of the system is met:

$$Q_{total\_system} = \sum_{j=1}^{g} Q_{Gk} + Q_{PV} = \sum_{j=1}^{g} \frac{1}{n_{qk}} (V_0 - V_k) + Q_{PV} \qquad (4.23)$$

Once the new frequency is calculated, the new admittance matrix is re-evaluated and Step 1 is repeated to get the new bus voltages. This process is repeated until the error between the new (i+1) and the old (i) values of the voltages and the angular frequency is less than the pre-specified error margin. In addition, the mismatch between the generated and consumed reactive power must be less than the error margin.

Figure 4.4-1 depicts a flowchart which shows the steps involved in the modified load flow algorithm. In addition, Appendix A presents the detailed load flow algorithm developed using MATLAB.

As can be seen from the flowchart below, in order to improve the convergence rate of the proposed algorithm, the initial educated guesses of the unknown variables are calculated using the conventional load flow algorithm. The latter initial values are then fed to the modified Gauss-Seidel algorithm. When running the conventional load flow algorithm, all droop-controlled generators are assumed to be operated in PV-mode. In addition, PQ buses and the elements of the admittance matrix are assumed to be insensitive to frequency variations.

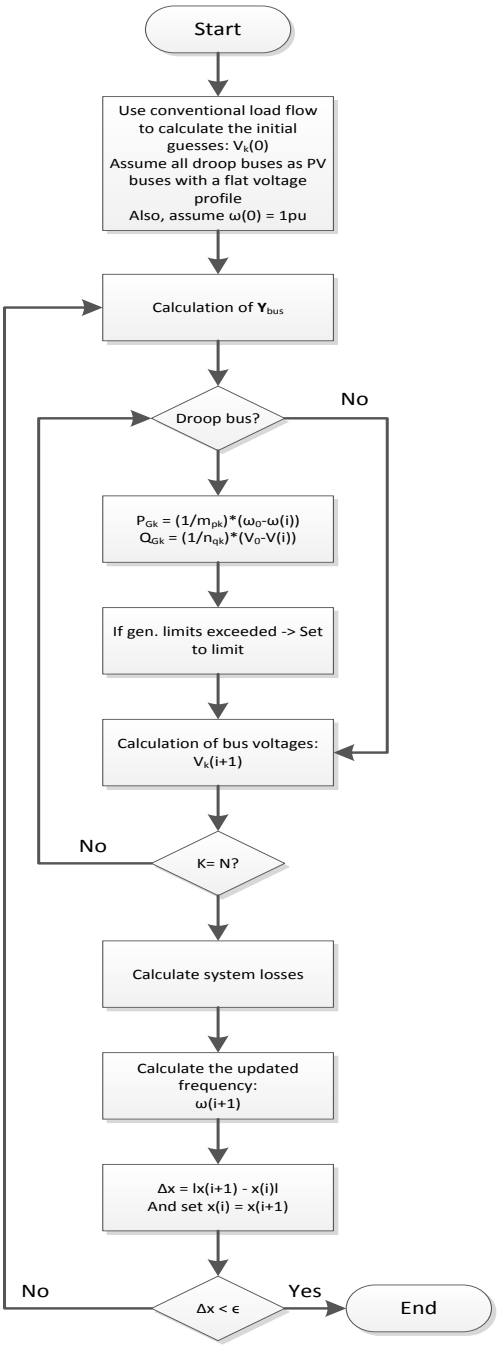

Figure 4.4-1 Flowchart of the Modified Load Algorithm[5]

[5] The notation (*i)* and (*i+1)* respectively denote old and current values (of either V or ω). The letter *N* is the total number of buses.

CHAPTER 5

SIMULATION RESULTS

5.1 Test System

The validity of the methodology presented above is tested on a six-bus microgrid system, comprising three distributed generators, two loads, and five feeders [23]. The technical characteristics of each microgrid element are given in Table 5.1-1 through Table 5.1-4.

The results of the microgrid load flow algorithm are compared against the values obtained through a time-domain simulation conducted using the software PSCAD. The metrics of interest are system frequency, voltage magnitudes and angles, total consumed load, and system ohmic losses. Two cases will be studied. In the first case the m_p factor is chosen to be very low so as to result in a system frequency that is close to 1pu. In the second case, the algorithm will be tested to see its accuracy when the frequency of the system is allowed to reach values that are closer to 0.95 pu. In the two cases the parameter n_p is kept constant at a pu value of 0.005909pu (which corresponds to 0.0013 V/VAr).

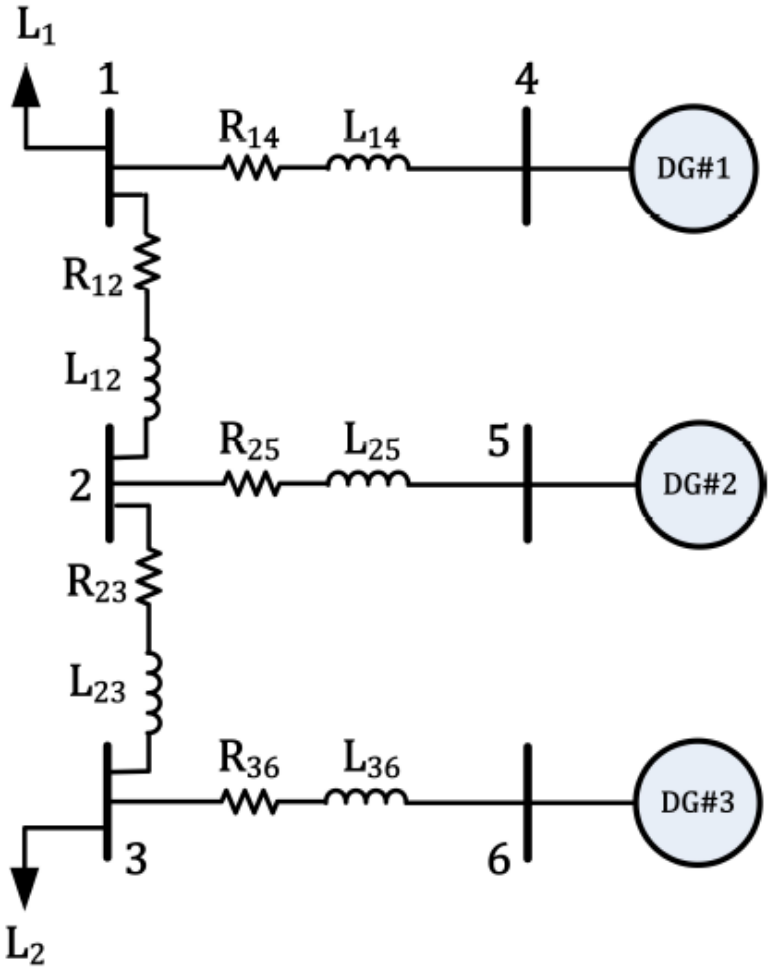

Figure 5.1-1 Six-Bus Benchmark Microgrid [15]

Table 5.1-1 PU Base Calculations

S_{base}, kVA	1
V_{base}, V (phase-phase)	220
Z_{base}, Ω	14.5161
f, Hz	60

Table 5.1-2 Generator Parameters

Identical DG units: 10 kVA (3-ph), 127 V (L-N), 60 Hz			
m_p (pu)	**n_q (pu)**	**w_{ref} (pu)**	**V_{ref} (pu)**
0.001583 (or 9.4 E-05, rad/s/W)	0.005909 (or 0.0013 V/VAr)	1	1

Table 5.1-3 Line Parameters of the Six-Bus Microgrid

Line parameters (per phase)			
From bus	**To bus**	**R_{line} (ohm)**	**L_{line} (mH)**
1	2	0.43	0.318
2	3	0.15	1.843
3	6	0.05	0.050
4	1	0.30	0.530
2	5	0.25	0.250

Table 5.1-4 Load Data

System Load, per phase		
Bus number	**R_L(Ω)**	**L_L(mH)**
1	6.95	12.2
2	0	0
3	5.014	9.4
4	0	0
5	0	0
6	0	0

5.2 Results: Load Flow

5.2.1 Constant Operating Parameters

This section presents the results pertaining to the six-bus benchmark system operating under the operating parameters presented in Table 5.1-1 to Table 5.1-4. It is evident from Figure 8 that conventional Gauss-Seidel load flow algorithm (CGS) does not capture the bahiour of droop-controlled buses and therefore yields inaccurate reults. It can be observed that voltage levels at droop-controlled buses vary with respect to system frequency. The latter is not feature is not at all captured when droop-controlled buses are modelled as PV-types buses.

5.2.1.1 Nominal Frequency Operation

Table 5.2-1 to Table 5.2-3 show a comparison of the results obtained from the Gauss-Seidel method and PSCAD. As these tables show, the results are in agreement as the difference between the two methods is always less than 0.54%. These error values are also very close to those obtained using the Newton-Raphson Trust-Region method that was adopted in [15]. In [15] the highest error value of voltage magnitudes was 0.5%.

Table 5.2-1 MGS v. PSCAD: Bus Voltages – High Frequency Operation

Bus Nbr.	Voltage Magnitude (pu)		Angle (Degrees)	
	MGS	PSCAD	MGS	PSCAD
1	0.9592	0.9566	0	0
2	0.9732	0.9704	-0.5501	-0.5605
3	0.9662	0.9610	-2.8126	-2.8719
4	0.9887	0.9861	-0.0832	-0.0877
5	0.9919	0.9893	-0.4561	-0.47778
6	0.9722	0.9670	-3.0679	-3.0702

Table 5.2-2 MGS v. PSCAD: Active and Reactive Power – Nominal Frequency Operation

Bus Nbr.	Active Power (pu)		Reactive Power (pu)	
	MGS	PSCAD	MGS	PSCAD
1	-4.8676	-4.8420	-3.200	-3.2040
2	0	0	0	0
3	-6.4765	-6.4350	-4.5431	-4.5480
4	3.8478	3.8529	1.8971	1.9259
5	3.8478	3.8529	1.3578	1.4781
6	3.8478	3.8529	4.7002	4.5635

Table 5.2-3 MGS v. PSCAD: System Frequency – Nominal Frequency Operation

System Frequency (pu)	
MGS	PSCAD
0.99905	0.99904

5.2.1.2 Reduced Frequency Operation

In this section reduced frequency operation of the system is tested and the results obtained with the proposed MGS algorithm are compared against their counterpart derived from a PSCAD simulation.

In order to capture a reduced frequency operation state, the active power static droop control (m_p) of all three droop-controlled DG unit is set to a value of 0.0135pu; the rest of system parameters are the same used in the preceding section.

As shown in Table 5.2-4 to Table 5.2-6, even when the system is operated at lower frequency levels (in this case around 57.11 Hz) the results of the proposed algorithm and those obtained using PSCAD are in good agreement. Indeed, the highest error is as low as 0.6%.

Table 5.2-4 MGS v. PSCAD: Bus Voltages – Reduced Frequency Operation

Bus Nbr.	Voltage Magnitude (pu)		Angle (Degrees)	
	MGS	PSCAD	MGS	PSCAD
1	0.9581	0.9601	0	0
2	0.9721	0.9733	-0.5432	-0.5412
3	0.9677	0.9734	-2.8397	-2.8297
4	0.9865	0.9879	-0.0854	-0.0854
5	0.9902	0.9917	-0.4329	-0.4421
6	0.9732	0.9786	-3.0563	-3.0488

Table 5.2-5 MGS v. PSCAD: Active and Reactive Power – Reduced Frequency Operation

Bus Nbr.	Active Power (pu)		Reactive Power (pu)	
	MGS	PSCAD	MGS	PSCAD
1	-4.4920	-4.4784	-2.9726	-2.9965
2	0	0	0	0
3	-5.9708	-5.9568	-4.2199	-4.2301
4	3.5792	3.5801	2.2695	2.2710
5	3.5792	3.5803	1.6545	1.6560
6	3.5792	3.5801	4.5220	4.5281

Table 5.2-6 MGS v. PSCAD: System Frequency – Reduced Frequency Operation

System Frequency (pu)	
MGS	PSCAD
0.95168	0.95170

5.2.1.3 Conventional Gauss-Seidel vs. Modified Gauss-Seidel Load Flow Algorithm

In order to show the relevance of using the modified Gauss-Seidel method (MGS) in isolated microgrid applications, Figure 5.2-1 compares the results obtained with the latter method to those calculated using CGS. Given that CGS does not allow the modeling of droop-controlled generators, the buses to which these generator types are connected are modelled as PV buses. PV buses are characterized by both a fixed active power and a fixed scheduled voltage. This makes PV buses completely insensitive to droop-control parameters (primarily the reactive power static droop n_q). In the example shown in Figure 5.2-1, the scheduled voltage was set to 1pu for all

generator PV buses. In addition, equal load active power sharing between the three generators was assumed: that is, each generator supplied one third of the total load. Finally, CGS load flow requires the selection of a slack bus; DG1 was selected as such. It is evident from Figure 5.2-1 that CGS algorithm does not capture the behaviour of droop-controlled buses and therefore yields inaccurate voltage levels. It can be observed that voltage levels at droop-controlled buses vary with respect to the selected reactive power static droop gain n_q. The latter feature is not captured when droop-controlled buses are modelled as PV-type buses.

Figure 5.2-1 clearly shows that for relatively high values of both m_p and n_q, the difference between the results obtained by CGS method and MGS method is further exacerbated. Higher values of m_p result in lower system frequencies in the case of the MGS, whereas the frequency is assumed constant in CGS. Reactive power injections of generators are reduced when high values of n_p are selected, which tend to further depress bus voltage magnitudes. These voltage depressions are not captured with CGS method because the latter assumes all generators to be connected to PV buses (hence, a constant active power and voltage magnitude).

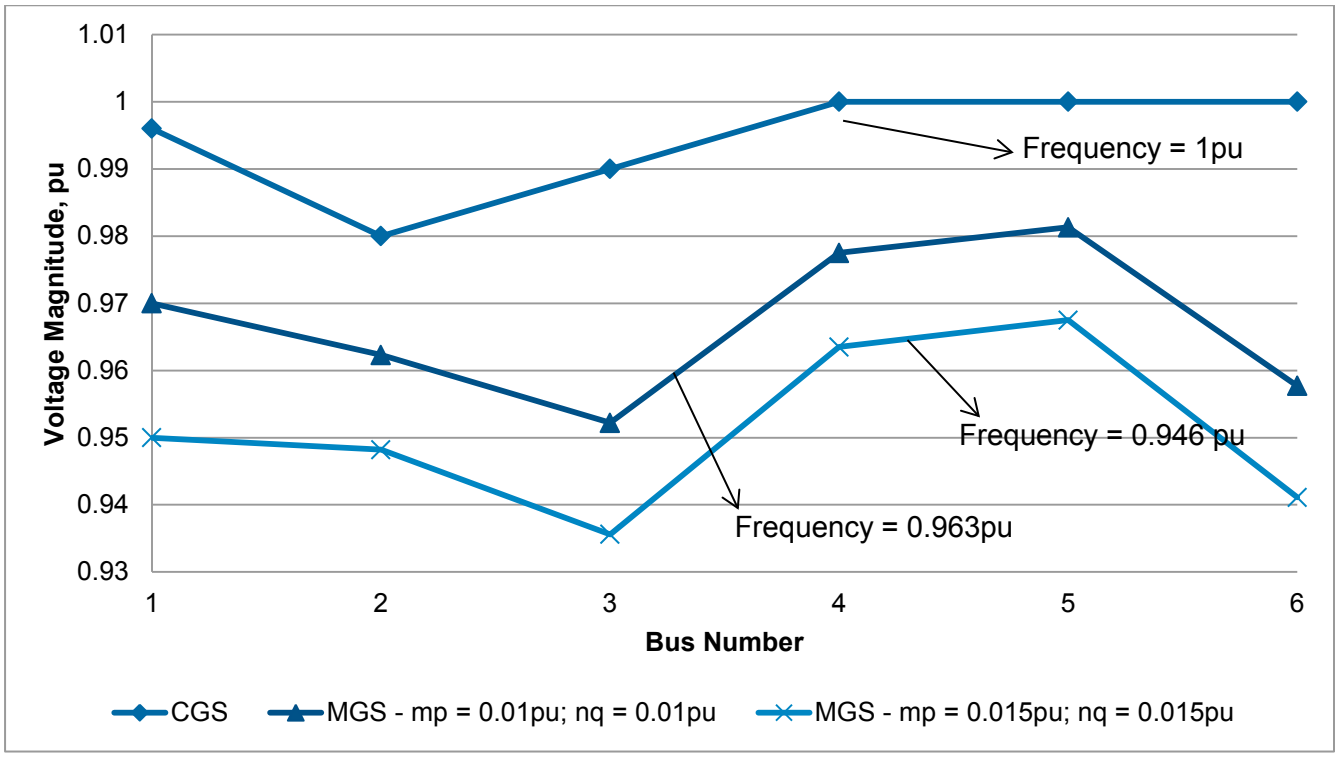

Figure 5.2-1 Result Comparison: MGS vs. CGS

5.2.2 Part II: Variable Operating Parameters

In order to further test the validity and the robustness of the proposed load flow algorithm, a number of operating parameters are varied and their effect on other variables is recorded. The following relationships are reported:

- Frequency vs. load variation;
- Bus voltage vs. load variation;
- Active and reactive power of generators vs. load variation;
- Bus voltages vs. n_q.

These tests help ensure that the theoretical relationships between the investigated variables is as expected.

5.2.3 Frequency vs. Load Variation

As explained in the preceeding sections, an increase in the load results in a proportional decrease in system frequency. As shown in Figure 5.2-2, when the total system load is randomnly varied from 6pu to 12pu over a 48 hour period, the fluctuation of the frequency is as expedted: 12pu loading yields the lowest system frequency, while 6pu loading results in the highest frequency level.

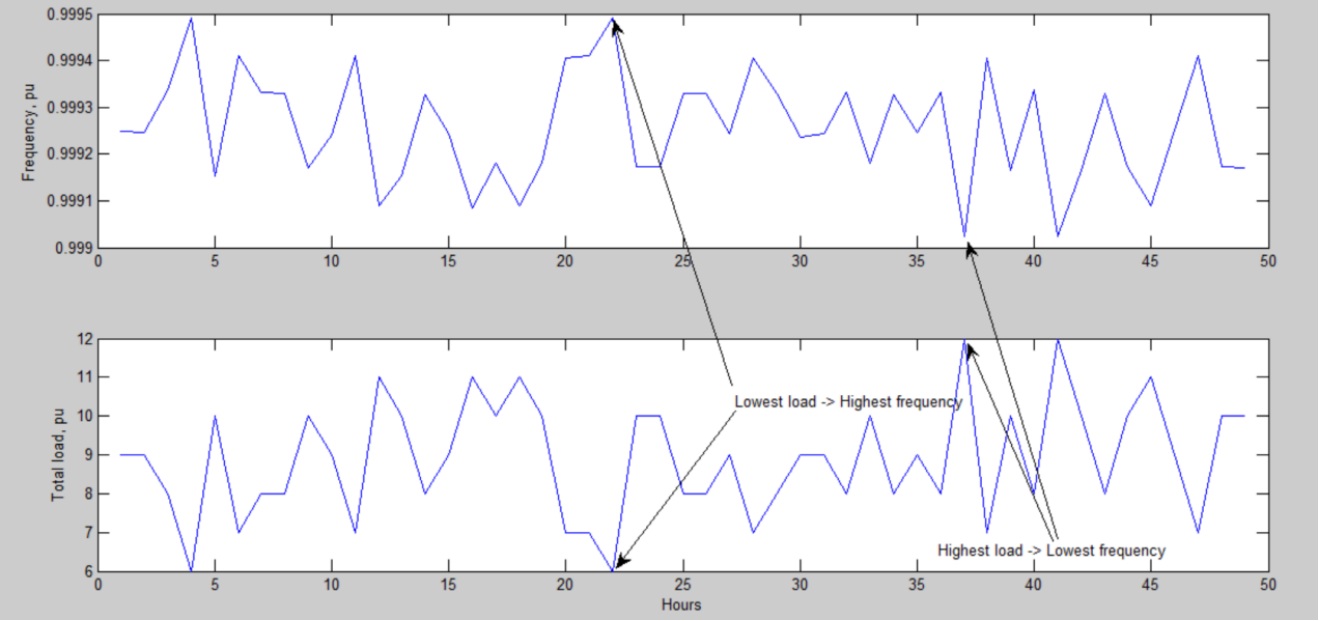

Figure 5.2-2 Variation of frequency with respect to load

5.2.4 Bus Voltage vs. Load Variation

Figure 5.2-3 shows the variation of bus voltage magnitudes with respect to system load. As expected, bus voltage magnitudes decrease as total system load increases, and vice versa.

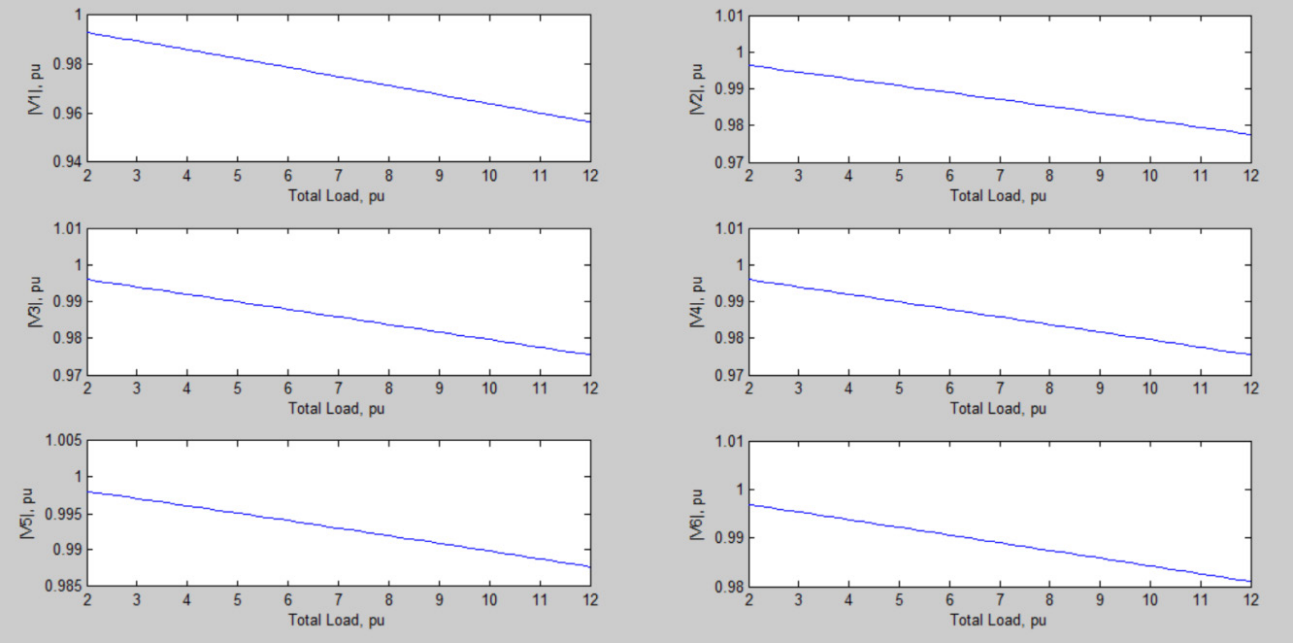

Figure 5.2-3 Bus Voltage vs. Total Load

5.2.5 Bus Voltage vs. n_q

This section examines the variation of bus voltages with respect to the reactive power static-droop gain, n_q. Apart from n_q the remaining variables are kept constant, as indicated in Table 5.1-1 to Table 5.1-4. As shown in Figure 5.2-4, the algorithm yields results that are in accordance with theory, i.e., the highest voltage magnitudes are achieved with the lowest and most charge-sensitive static droop gains.

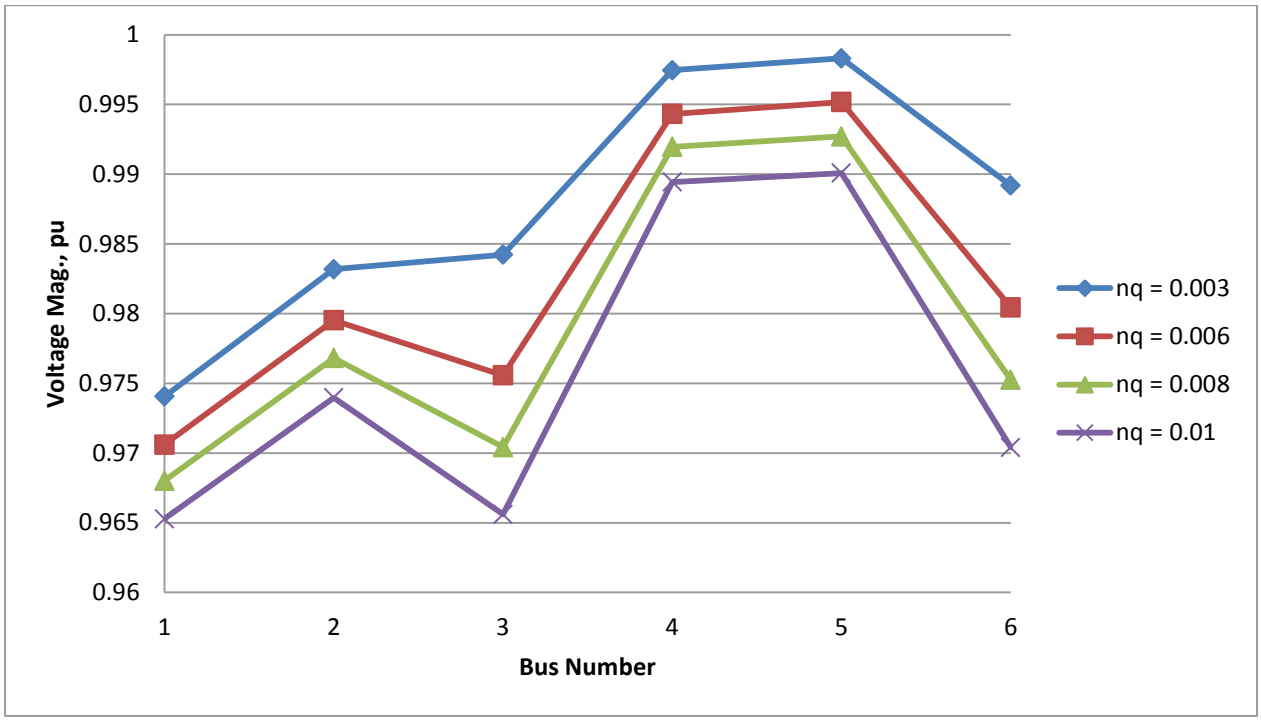

Figure 5.2-4 Variation of bus voltages with respect to n_q

5.2.6 Frequency vs. m_p

Apart from n_q the remaining variables are kept constant, as indicated in Table 5.1-1 to Table 5.1-4. In examining frequency in relation to m_p, the theoretical results are further confirmed. As can be seen in Figure 5.2-5, the highest system frequencies are obtained when the active power static droop control parameter, m_p, is at its lowest, least sensitive values. As can be derived from equation (4.8), the lowest values of m_p result in the highest active power output of the DG unit, which results in the highest system frequency. Therefore if a system has the capacity to operate at frequencies lower than 1pu (for example, possible operation at 0.95pu or less), then relatively high values of m_p can be envisaged, leading to lower DG unit outputs, which in turn result in

lower generation cost. These findings are particularly important since frequency changes resulting from the variation of m_p cannot be captured by conventional load flow algorithms.

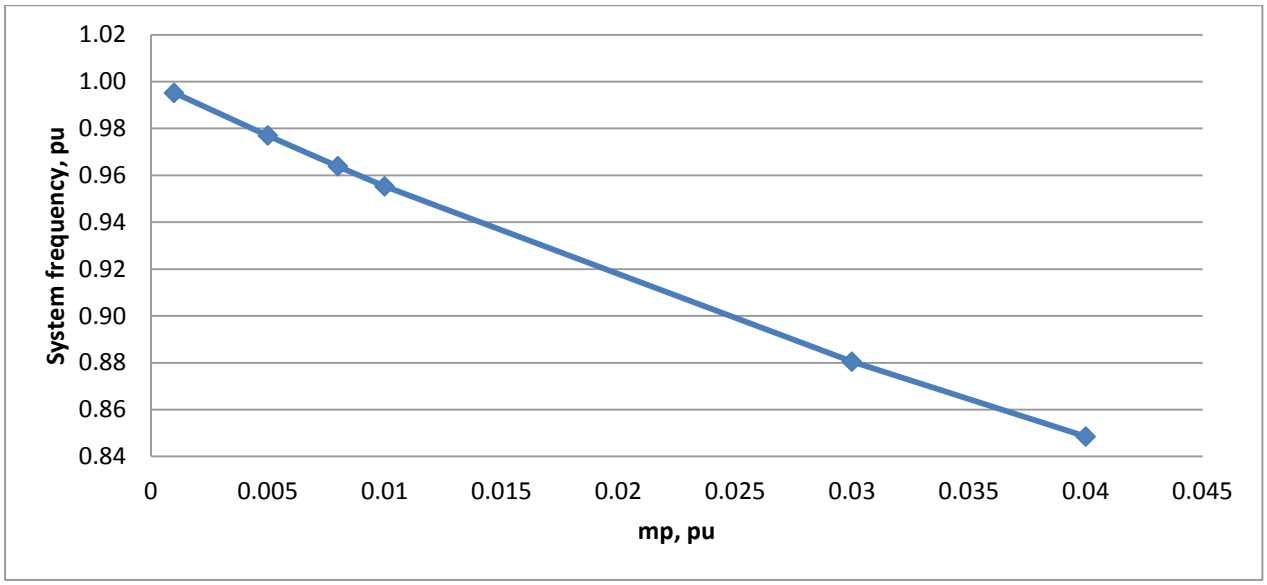

Figure 5.2-5 Variation of system frequency with respect to m_p

5.3 Discussion

5.3.1 Load Flow Problem

This thesis proposed a load flow algorithm to model the operation of balanced islanded microgrids. In order to mimic fully the off-grid operation, no slack bus was resorted to, given that the size of generators in a microgrid is never big enough to assume the role of a slack generator. The three generators of the studied system (Figure 5.1-1) were modeled as droop-controlled buses, while the loads were modeled as PQ buses. The results obtained using the proposed algorithm showed perfect agreement with the results obtained using time-domain simulation software. The proposed algorithm is a valuable tool to study the operation of islanded microgrids, especially from a planning perspective when there is a need for the expansion of a

microgrid (i.e., the increase of the load, addition of generators, etc.). The proposed algorithm allows for the efficient study of different reliability aspects of the system, such as steady-state voltage stability, loading levels of the various feeders, and frequency variation.

CONCLUSION AND FUTURE WORK

6.1 Conclusion

The main focus of this thesis is primarily related to various planning aspects of microgrids. When planning an electric network, two major operating states are considered: steady-state and dynamic operation. This thesis covered the steady-state aspect, which is chiefly concerned with voltage stability, loading levels of the feeders, as well as the operation within accepted frequency limits. These aspects are investigated through a thorough steady-state analysis which relies on load flow algorithms.

Whenever a microgrid is envisaged, it is crucial to study it under islanded operation. Islanded operation is the most constraining condition when the microgrid is completely disconnected from the main grid. This fact makes it necessary for the microgrid to regulate its own voltage levels as well as its frequency while meeting load demand. In order to achieve this goal, DG units in microgrids are usually operated in droop-control mode. Under this mode of operation, the output active power of the DG units is not set to a pre-specified value but rather adjusted with respect to changes in system frequency. Similarly, the reactive power output of these generators is calibrated against the voltage level at the connecting bus. Since the complexity of droop-control is not accounted for when conventional load flow algorithms are applied to isolated microgrids, these algorithms lead to very inaccurate and rather misleading load flow results.

The load flow algorithm proposed in this thesis allows to simulate all aspects of droop-controlled islanded microgrids in steady-state operation. The results of the algorithm were in perfect agreement with those obtained using time-domain simulation tools.

6.2 Future Work

The algorithm developed in this thesis is a good start in the study of microgrids operated in off-grid mode. However, a number of other aspects should be addressed in future works covering the same topic:

- The fact that many microgrids operate in an unbalanced mode (given the nature of the loads which they feed) makes it necessary to develop a three-phase load flow algorithm to tackle unbalanced operation.
- Beyond the calculation of production costs, an algorithm should also be developed to optimally dispatch the generators in a microgrid. The optimal dispatch is an optimization problem which tends to minimize the production cost of an electric system by making use of the least expensive available generation.

REFERENCES

[1] F. Blaabjerg, Z. Chen, and S. B. Kjaer. ”Power electronics as efficient interface in dispersed power generation systems”. IEEE Transactions On Power Electronics, 19(5):1184 – 1194, 2004.

[2] R. H. Lasseter, "Smart Distribution: Coupled Microgrids," Proceedings of the IEEE , vol. 99, no. 6, pp. 1074-1082, Jun. 2011.

[3] R. Palma-Behnke, L. Reyes and G. Jimenez-Estevez, "Smart grid solutions for rural areas," in IEEE 2012 Power and Energy Society General Meeting, 2012, pp. 1-6.

[4] Klaus Heuk, Klaus-Dieter Dettman, “Elektrische Energieversorgung”, Vieweg, 3rd Edition.

[5] John W. Simpson-Porco, Florian D¨orfler, Francesco Bullo, “Synchronization and Power Sharing for Droop-Controlled Inverters in Islanded Microgrids”, University of California, Santa Barbara.

[6] S. Chowdhury, S.P. Chowdhury, P. Crossley, “Microgrids and Active Distribution Networks”, IET Renewable Energy Series 6, 2009.

[7] IEEE Std. 1547.4, “IEEE Guide for Design, Operation, and Integration of Distributed Resource Island Systems with Electric Power Systems,” IEEE Standards Coordinating Committee 21, 2011.

[8] ABB User Manual: Renewable Microgrid Controller MGC600.

[9] Lianqing Zheng, Chen Zhuang, Jian Zhang and Xiong Du, “An Enhanced Droop Control Scheme for Islanded Microgrids,” International Journal of Control and Automation, Vol. 8, No. 4, pp. 63-74, 2015.

[10] P. Kundur, “Power system loads,” in Power System Stability and Control. New York: McGraw-Hill, 1994, ch. 7, pp. 271-314.

[11] P. Kundur, Power System Stability and Control. New York: McGraw-Hill, 1994, ch. 8.

[12] N. Pogaku, M. Prodanovic and T. C. Green, "Modeling, analysis and testing of autonomous operation of an inverter-based microgrid," IEEE Trans. Power Electron., vol. 22, no. 2, pp. 613-625, Mar. 2007.

[13] M. Z. Kamh and R. Iravani, “Unbalanced model and power-flow analysis of microgrids and active distribution systems,” *IEEE Trans. Power Del.*, vol. 25, no. 4, pp. 2851–2858, Oct. 2010.

[14] H. Nikkhajoei and R. Iravani, “Steady-state model and power flow analysis of electronically-coupled distribution resource units,” *IEEE Trans. Power Del.*, vol. 22, no. 1, pp. 721–728, Jan. 2007.

[15] Morad Mohamed Abdelmageed Abdelaziz, “A Novel and Generalized Three-Phase Power Flow Algorithm for Islanded Microgrids Using a Newton Trust Region Method,” IEEE Transactions on Power Systems, February 2015.

[16] Faisal Mumtaz, M. Syed, Mohamed Al Hosani, H. H. Zeineldin, “A simple and accurate approach to solve the power flow for balanced islanded microgrids,” IEEE Conference Publication, pp. 1852 – 1856, 2015.

[17] El-Hawary M.E., Christensen G.S., “Optimal Economic Operation of Electric Power Systems,” New York, NY, US; Academic Press, 1979.

[18] “Load representation for dynamic performance analysis of power systems,” Power Systems, IEEE Transactions on, vol. 8, no. 2, pp.472–482, May 1993.

[19] N. Pogaku, M. Prodanovic and T. C. Green, "Modeling, analysis and testing of autonomous operation of an inverter-based microgrid," IEEE Trans. Power Electron., vol. 22, no. 2, pp. 613-625, Mar. 2007.

[20] J. M. Guerrero, L. G. De-Vicuna, J. Matas, M. Castilla and J. Miret, "Output impedance design of parallel-connected UPS inverters with wireless load-sharing control," IEEE Trans. Ind. Electron., vol. 52, no. 4, pp. 1126-1135, Aug. 2005.

[21] ANSI/NEMA C84.1, “American National Standard for Electric Power Systems and Equipment— Voltage Ratings (60 Hertz),” 2006.

[22] Andrew J. Roscoe, Graeme M. Burt and Chris G. Bright, “Avoiding the Non-Detection Zone of Passive Loss-of-Mains (Islanding) Relays for Synchronous Generation by using Low Bandwidth Control Loops and Controlled Reactive Power Mismatches,” IEEE Transactions on Smart Grids.

[23] S.K. Chaudhury, Josep M. Guerrero, J.C. Vasquez, “Power Flow Analysis Algorithm for Islanded LV Microgrids Including Distributed Generator Units with Droop Control and Virtual Impedance Loop”, March 2014.

[24] Eleonora Riva Sanseverino, Maria Luisa Di Silvestre, Romina Badalamenti, Ninh Quang Nguyen, Josep Maria Guerrero, Lexuan Meng, “Optimal Power Flow in Islanded Microgrids Using a Simple Distributed Algorithm,” Energies, 2015, ISSN 1996-1073.

[25] Changsun Ahn and Huei Peng, “Decentralized and Real-Time Power Dispatch Control for an Islanded Microgrid Supported by Distributed Power Sources,” Energies, 2013, ISSN 1996-1073.

[26] A. Micallef, M. Apap, C. Spiteri-Staines, and J. M. Guerrero, “Secondary Control for Reactive Power Sharing in Droop-Controlled Islanded Microgrids.”

[27] British Standard BS 7671, “Requirements for Electrical Installations, IET Wiring Regulations.”

APPENDIX A

Load Flow Algorithm: MATLAB Code

% Bus data

```
% Bus Data for Load Flow Analysis.
%This M-file evaluates the parameters of generators and loads connected to all buses in the system

function busdata = busdatan(Sb,Vb,wb)

j=sqrt(-1);
Zb=Vb^2/Sb;

%%%%%%%%%%%%%%%%%%%%%%%%%%%%%%%%%%%%%%%%%%%%%%%%%%%%%%%%%%%%%%%%%%%%%
%Load Power Factor
pf = 0.9;
%%%%%%%%%%%%%%%%%%%%%%%%%%%%%%%%%%%%%%%%%%%%%%%%%%%%%%%%%%%%%%%%%%%%%
%Load @ Bus1
  Zl01pu=(6.95+j*12.2e-3*wb)/Zb;
  Pl01=real(1/Zl01pu);
  Ql01=-imag(1/Zl01pu);
%%%%%%%%%%%%%%%%%%%%%%%%%%%%%%%%%%%%%%%%%%%%%%%%%%%%%%%%%%%%%%%%%%%%%
% Load @ Bus3
  Zl03pu=(5.014+j*9.4e-3*wb)/Zb;
  Pl03=real(1/Zl03pu);
  Ql03=-imag(1/Zl03pu);

%Parameters of Droop-Controlled Generators
mp = 0.001583;
nq = 0.005905;


P=4000/Sb;Q=3000/Sb;
%       |Bus | Type | Vsp | theta | PGi | QGi | PLi | QLi |PGmin | PGmax|
busdata1 = [1    3   220/Vb   0    0     0    Pl01  Ql01    0    0;
        2    3   220/Vb   0    0     0    Pl02  Ql02    0    0;
        3    3   220/Vb   0    0     0    Pl03  Ql03    0    0;
        4    2   220/Vb   0    P     Q     0    0     0  6000/Sb;
        5    2   220/Vb   0    P     Q     0    0     0  6000/Sb;
        6    2   220/Vb   0    0     0     0    0     0  6000/Sb];

    %        | QGmin | QGmax | Frequency Droop coeff.| Voltage  Droop coeff. |
busdata2 = [ 0      0         0                  0;
          0      0         0                  0;
          0      0         0                  0;
          0   5000/Sb      mp                 nq;
          0   5000/Sb      mp                 nq;
          0   5000/Sb      mp                 nq];

busdata=[busdata1,busdata2];
```

% Admittance Matrix

```
function [ybus,ldata] = ybusppg(w,Zb)

j=sqrt(-1);

linedata = linedatam(w,Zb);
fb = linedata(:,1);     % From bus number
tb = linedata(:,2);     % To bus number
r = linedata(:,3);      % Resistance, R
x = linedata(:,4);      % Reactance, X
b = linedata(:,5);      % Ground Admittance, B/2
z = r + j*x;            % Z matrix...
y = 1./z;               % To get inverse of each element
b = j*b;                % Make B imaginary
ldata=[fb,tb,z,r,x];

nbus = max(max(fb),max(tb));    % no. of buses
nbranch = length(fb);           % no. of branches
ybus = zeros(nbus,nbus);        % Initialize YBus

 % Off Diagonal Elements
 for k=1:nbranch,
    ybus(fb(k),tb(k)) = -y(k);
    ybus(tb(k),fb(k)) = ybus(fb(k),tb(k));
 end

 % Diagonal Elements
 for m=1:nbus,
    for n=1:nbranch,
       if ((fb(n) == m) || (tb(n) == m)),
          ybus(m,m) = ybus(m,m) + y(n) + b(n);
       end
    end
 end
```

% Line Data

```
function linedata = linedatam(w0,Zb)

%        | From |  To  |     R    |      X        |   B/2 |
%        |  Bus  | Bus  |          |               |       |
linedata = [ 1       2    0.43/Zb    0.000318*w0/Zb     0;
             1       4    0.30/Zb    0.000350*w0/Zb     0;
             2       3    0.15/Zb    0.001843*w0/Zb     0;
             2       5    0.20/Zb    0.000250*w0/Zb     0;
             3       6    0.05/Zb    0.000050*w0/Zb     0];
```

```
% Conventional Gauss - Seidel Load Flow Analysis

function [GenpuMW,GenpuMVAR,V] = GSTraditional(Sbase,Vbase,wbase)

%%%%%%%%%%%%%%%%%%%%%%%%%%%%
Zbase=Vbase^2/Sbase;
Vnominal=1;            % Nominal Voltage in p.u.
%%%%%%%%%%%%%%%%%%%%%%%%%%%%
 busdata = busdatan(Sbase,Vbase,wbase);
bus = busdata(:,1);     % Bus Number                                          .
type = busdata(:,2);    % Type of Buses: 1-Droop, 2-PV, 3-PQ
V = busdata(:,3);       % Initial Bus Voltages.
th = busdata(:,4);      % Initial Bus Voltage Angles.
GenpuMW = busdata(:,5);   % PGi, Real Power injected into the buses.
GenpuMVAR = busdata(:,6); % QGi, Reactive Power injected into the buses.
LoadpuMW = busdata(:,7);  % PLi, Real Power Drawn from the Buses.
LoadpuMVAR = busdata(:,8);% QLi, Reactive Power Drawn from the Buses.
Pgmin = busdata(:,9);   % Minimum Active Power Limit
Pgmax = busdata(:,10);  % Maximum Active Power Limit
Qgmin = busdata(:,11);  % Minimum Reactive Power Limit
Qgmax = busdata(:,12);  % Maximum Reactive Power Limit

mp = busdata(:,13);     % Frequency Droop Coefficient
nq = busdata(:,14);     % Voltage Droop Coefficient
nbus = max(bus);
P = GenpuMW - LoadpuMW;     % Pi = PGi - PLi, Real Power at the Buses.
Q = GenpuMVAR - LoadpuMVAR; % Qi = QGi - QLi, Reactive Power at the Buses.

Vspec=zeros(nbus,1);
for b1=1:nbus,
   if (type(b1) ~= 3),
      Vspec(b1)=V(b1);
   end
end

Vprev = V;
w0=wbase;

[ybus,ldata] = ybusppg(w0,Zbase);

wb=w0/wbase;
iteration = 0;
toler = 1;
j=sqrt(-1);
```

```
%%%%%%%%%%%%%%%%%% Main Loop %%%%%%%%%%%%%%%%%%

while (toler > 1e-7)

%%%%%%%%%%%% Bus Voltage Calculation
 for i1 = 1:nbus-1,
       sumyv = 0;
       for k = 1:nbus,
          if i1 ~= k,
             sumyv = sumyv + ybus(i1,k)* V(k);  % Vk * Yik
          end
       end

 V(i1)=(1/ybus(i1,i1))*((P(i1)-j*Q(i1))/conj(V(i1))-sumyv);

 end

 for i1 = 1:nbus-1,

% Update of PV Buses %%%%%%%%%%%%%%%%%
       sumyv = 0;
       for k = 1:nbus
          if i1 ~= k,
             sumyv = sumyv + ybus(i1,k)* V(k);
          end
       end
       if (type(i1) == 2),
          Q(i1) = -imag(conj(V(i1))*(sumyv + ybus(i1,i1)*V(i1)));
             if Q(i1) < Qgmin(i1)-LoadpuMVAR(i1),
                Q(i1) = Qgmin(i1)-LoadpuMVAR(i1);
                V(i1)=(1/ybus(i1,i1))*((P(i1)-j*Q(i1))/conj(V(i1))-sumyv);
             end
             if Q(i1) > Qgmax(i1)-LoadpuMVAR(i1),
                Q(i1) = Qgmax(i1)-LoadpuMVAR(i1);
                V(i1)=(1/ybus(i1,i1))*((P(i1)-j*Q(i1))/conj(V(i1))-sumyv);
             end
             if (Q(i1) <= Qgmax(i1)-LoadpuMVAR(i1)),
                if (Q(i1) >= Qgmin(i1)-LoadpuMVAR(i1)),
                   V(i1)=abs(Vspec(i1))*cos(angle(V(i1)))+...
                        j*abs(Vspec(i1))*sin(angle(V(i1)));
                end
             end
       end
 end
```

```
iteration = iteration + 1;

   toler = max(abs(Vprev-V));
   Vprev = V;

end


%  System loss calculation
Ilines =(V(ldata(:,1))-V(ldata(:,2)))./(ldata(:,3));
Ploss=sum(ldata(:,4).*abs(Ilines).^2);
Qloss=sum(ldata(:,5).*abs(Ilines).^2);

% Slack bus
GenpuMW(6)=sum(LoadpuMW)+Ploss-sum(GenpuMW);
GenpuMVAR(6)=sum(LoadpuMVAR)+Qloss-sum(GenpuMVAR);

iteration;
V;
Vmag = abs(V);
Ang = 180/pi*angle(V);
PolV=[Vmag,Ang];
```

```
% Modified Gauss - Seidel Load Flow Analysis

Sbase=1000;  % Base VA
Vbase=220;   % Base Voltage
wbase=2*pi*60;
Zbase=Vbase^2/Sbase;
Vnominal=1;

% Initial Guess from Conventional LF Algorithm
[Pgst,Qgst,Vgst] = GSTraditional(Sbase,Vbase,wbase);

busdata = busdatan(Sbase,Vbase,wbase);
bus = busdata(:,1);     % Bus Number.
type = busdata(:,2);    % Type of Buses: 2-Droop, 3-PQ (No Slack Bus)
V = busdata(:,3);           % Initial Bus Voltages.
th = angle(Vgst);        % Initial Bus Voltage Angles.
GenpuMW = Pgst;          % PGi
GenpuMVAR = Qgst;        % QGi
LoadpuMW0 = busdata(:,7);  % PLi
LoadpuMVAR0 = busdata(:,8);% QLi
Pgmin = busdata(:,9);   % Minimum Active Power Limit
Pgmax = busdata(:,10);  % Maximum Active Power Limit
Qgmin = busdata(:,11);  % Minimum Reactive Power Limit
Qgmax = busdata(:,12);  % Maximum Reactive Power Limit
kp=1.5;kq=1.5;         % Load Cofficients
P = GenpuMW - LoadpuMW0;     % Pi = PGi - PLi
Q = GenpuMVAR - LoadpuMVAR0; % Qi = QGi - QLi

mp = busdata(:,13);
nq = busdata(:,14);
nbus = max(bus);

sig1pmp=0;
sig1pnq=0;
ndroop=0;


for i1=1:max(bus),
   if ((type(i1) == 1) || (type(i1) == 2)),
      type(i1)=2;
      sig1pmp=sig1pmp+1/mp(i1);
      sig1pnq=sig1pnq+1/nq(i1);
      ndroop=ndroop+1;
   end
end
```

```
Vspec=V;
for b1=1:nbus,
   if (type(b1) ~= 3),
      Vspec(b1)=V(b1);
   end
end

Vprev = Vgst;

w0=wbase;
wb=w0/wbase;

w=0.99*w0/wbase;
iteration = 0;
toler = 1;
j=sqrt(-1);

while (toler > 1e-5)

V(4)=abs(V(4));

% Load Power Update
LoadpuMW=LoadpuMW0*(1+kp*wb*(w-1));
LoadpuMVAR=LoadpuMVAR0*(1+kq*wb*(w-1));

%  Ybus Update
 [ybus,ldata] = ybusppg(w*wbase,Zbase);

 %%%%%%%%%%%%% Update of Droop Buses %%%%%%%%%%%%%%%%%%
for i1 = 1:nbus,
      sumyv = 0;
      for k = 1:nbus
         if i1 ~= k,
            sumyv = sumyv + ybus(i1,k)* V(k);
         end
      end
      if ((type(i1) == 2)),
            P(i1)=(wb-w)/mp(i1)-LoadpuMW(i1);
            Q(i1)=(abs(Vspec(i1))-abs(Vprev(i1)))/nq(i1)-LoadpuMVAR(i1);

            if P(i1) < Pgmin(i1)-LoadpuMW(i1),
               P(i1) = Pgmin(i1)-LoadpuMW(i1);
            end

            if P(i1) > Pgmax(i1)-LoadpuMW(i1),
               P(i1) = Pgmax(i1)-LoadpuMW(i1);
            end
```

```
            if Q(i1) < Qgmin(i1)-LoadpuMVAR(i1),
               Q(i1) = Qgmin(i1)-LoadpuMVAR(i1);
            end
            if Q(i1) > Qgmax(i1)-LoadpuMVAR(i1),
               Q(i1) = Qgmax(i1)-LoadpuMVAR(i1);
            end

      end
end

 %Voltage Calculation
 for i1 = 1:nbus,
      sumyv = 0;
      for k = 1:nbus,
         if i1 ~= k,
            sumyv = sumyv + ybus(i1,k)* V(k);
         end
      end
  V(i1)=(1/ybus(i1,i1))*((P(i1)-j*Q(i1))/conj(V(i1))-sumyv);
  if (i1==3),
     P(i1) = GenpuMW(i1) - LoadpuMW(i1);
     Q(i1) = GenpuMVAR(i1) - LoadpuMVAR(i1);
  end

 end
  V(4)=abs(V(4));


 % System Loss Calculation
Ilines =(V(Idata(:,1))-V(Idata(:,2)))./(Idata(:,3));
Ploss=sum(Idata(:,4).*abs(Ilines).^2);

  %Frequency Update
  wc=wb-(Ploss+sum(LoadpuMW))/sig1pmp;

iteration = iteration + 1;

% Tolerance Calculation
   toler = max([abs(Vprev-V);abs(wc-w)]);

   Vprev = V;
   w=wc;
end
```